
DECAYING MOMENTUM HELPS NEURAL NETWORK TRAINING

John Chen

Department of Computer Science
Rice University
Houston, Texas
johnchen@rice.edu

Cameron Wolfe

Department of Computer Science
Rice University
Houston, Texas
wolfe.cameron@rice.edu

Zhao Li

School of Biomedical Informatics
UTHealth
Houston, Texas
Zhao.Li@uth.tmc.edu

Anastasios Kyrillidis

Department of Computer Science
Rice University
Houston, Texas
anastasios@rice.edu

January 6, 2022

ABSTRACT

Momentum is a simple and popular technique in deep learning for gradient-based optimizers. We propose a decaying momentum (DEMON) rule, motivated by decaying the total contribution of a gradient to all future updates. Applying DEMON to Adam leads to significantly improved training, notably competitive to momentum SGD with learning rate decay, even in settings in which adaptive methods are typically non-competitive. Similarly, applying DEMON to momentum SGD improves over momentum SGD with learning rate decay in most cases. Notably, DEMON momentum SGD is observed to be significantly less sensitive to parameter tuning than momentum SGD with learning rate decay schedule, critical to training deep neural networks in practice. Results are demonstrated across a variety of settings and architectures, including image classification, generative models, and language models. DEMON is trivial to implement, easy to tune, and incurs limited extra computational overhead, compared to the vanilla counterparts. Code is readily available.

1 Introduction

Deep Neural Networks (DNNs) have advanced the state-of-the-art in computer vision [1, 2, 3], natural language processing [4, 5, 6] and speech recognition [7, 8], but have come with huge computation costs. A state-of-the-art language model can cost several million USD to train [9, 10]. For most practitioners and researchers, even moderate tasks, such as image classification on ImageNet, can be prohibitive in time and cost when the hyperparameter tuning process is taken into account, where it is typical to retrain models many times to achieve optimal performance. In the face of such significant developments, stochastic gradient descent (SGD) and accelerated SGD with momentum (SGDM) remain one of the most, if not the most, popular methods for training DNNs [11, 12, 13].

In an effort to ease the cost of training DNNs, adaptive methods [14, 15, 16, 17, 18] were devised. However, there are cases where their use leads to a performance gap [13, 19]. As a result, SGDM remains the optimizer of choice and state-of-the-art performance on many benchmarks—such as the image classification dataset ImageNet—is produced with SGDM [1, 2, 20, 21, 22, 3, 23].

For optimizers, including SGDM, to achieve good performance, their hyperparameters must be tuned properly. Slight changes in learning rate, learning rate decay, momentum, and weight decay (amongst others) can drastically alter performance. Hyperparameter tuning is extremely time consuming, and researchers often resort to a costly grid search. *Thus, the holy grail is achieving the performance and efficiency of SGDM with decreased dependence on hyperparameter tuning.*

The focus of this work is on how we can boost performance and reduce dependency on hyperparameter tuning with a simple technique for the momentum parameter. Momentum was designed to speed up learning in directions of low curvature, without becoming unstable in directions of high curvature. To minimize the objective function $\mathcal{L}(\cdot)$, the most common momentum method, SGDM, is given by the following recursion for variable vector $\theta_t \in \mathbb{R}^p$:

$$\theta_{t+1} = \theta_t + \eta v_t, \quad v_t = \beta v_{t-1} - g_t.$$

where β controls the rate of momentum decay, g_t represents a stochastic gradient, usually $\mathbb{E}[g_t] = \nabla \mathcal{L}(\theta_t)$, and $\eta > 0$ is the step size.

Practitioners usually set $\beta = 0.9$. This setting is supported by recent works that prescribe it [24, 17, 16, 25], and by the fact that most common softwares, such as PyTorch [26], use $\beta = 0.9$ as the default momentum value. There is no indication that this choice is universally well-behaved.

There are papers that attempt to tune the momentum parameter. In the distributed setting, [27] observe that running SGD asynchronously is similar to adding a momentum-like term to SGD. They provide empirical evidence that setting $\beta = 0.9$ results in a momentum “overdose”, yielding suboptimal performance. Additionally, YellowFin [28] is a learning rate and momentum adaptive method for both synchronous and asynchronous settings, motivated by a quadratic model analysis and some robustness insights. Finally, in training generative adversarial networks (GANs), optimal momentum values tend to decrease from $\beta = 0.9$ [29, 30, 31], taking even negative values [32].

In this paper, we introduce a novel momentum decay rule which significantly surpasses the performance of both Adam and SGDM in their current form (and other state-of-the-art adaptive learning rate and momentum methods), while provably increasing robustness to hyperparameters. Our findings can be summarized as follows:

- We propose a new momentum decay rule, motivated by decaying the total contribution of a gradient to all future updates, with limited overhead and additional computation.
- Adding the momentum decay rule to vanilla Adam, we observe large performance gains. The network continues to learn for far longer after Adam begins to plateau, suggesting that the momentum decay rule should be used as default for this method.
- We observe improved performance for SGDM with momentum decay over learning rate decay; an interesting result given the unparalleled effectiveness of learning rate decay.
- We show that optimizers with momentum decay are less sensitive to hyperparameters.

Experiments are provided on various datasets—including MNIST, FMNIST, CIFAR-10, CIFAR-100, STL-10, Tiny ImageNet, Penn Treebank (PTB); and networks—including Convolutional Neural Networks (CNN) with Residual architecture (ResNet) [2], Wide Residual architecture (Wide ResNet) [21], Non-Residual architecture (VGG-16) [33], Recurrent Neural Networks (RNN) with Long Short-Term Memory architecture (LSTM) [34], Variational AutoEncoders (VAE) [35], Capsule Network [36] and the recent Noise Conditional Score Network (NCSN) [37].

2 Preliminaries

Plain stochastic gradient descent motions. Let $\theta_t \in \mathbb{R}^p$ be the parameters of the network at time step t , where $\eta \in \mathbb{R}$ is the learning rate, and g_t is the stochastic gradient w.r.t. θ_t for empirical loss $\mathcal{L}(\cdot)$, such that $\mathbb{E}[g_t] = \nabla \mathcal{L}(\theta_t)$. Then, plain stochastic gradient descent (SGD) uses the recursion: $\theta_{t+1} = \theta_t - \eta \cdot g_t$, $\forall t$. Here, the step size η could be time dependent, η_t , but decreasing η at regular or predefined intervals works favorably in practice compared to decreasing η at every iteration.

SGDM is parameterized by $\beta \in \mathbb{R}$, the momentum coefficient, and follows the recursion:

$$\theta_{t+1} = \theta_t + \eta v_t, \quad v_t = \beta v_{t-1} - g_t,$$

where $v_t \in \mathbb{R}^p$ accumulates momentum. Observe that for $\beta = 0$, the above recursion is equivalent to SGD. Common values for β are closer to one, with $\beta = 0.9$ the most used value [38].

Adaptive gradient descent motions. These algorithms utilize current and past gradient information to design preconditioning matrices that better approximate the local curvature of $\mathcal{L}(\cdot)$. Beginning with AdaGrad [14], the update per coordinate i of θ , becomes:

$$\theta_{t+1,i} = \theta_{t,i} - \frac{\eta}{\sqrt{G_{t,ii} + \varepsilon}} \cdot g_{t,i}, \quad \forall t,$$

where $G_t \in \mathbb{R}^{p \times p}$ is usually a diagonal preconditioning matrix that sums the squares of past gradients and $\varepsilon > 0$ is a small constant.

RMSprop [16] substitutes the ever-accumulating matrix G_t with a root mean squared operation. Denoting the average of squared gradients as $\mathcal{E}_t^{g \circ g}$, per iteration we compute: $\mathcal{E}_{t+1}^{g \circ g} = \beta_2 \cdot \mathcal{E}_t^{g \circ g} + (1 - \beta_2) \cdot (g_t \circ g_t)$, where β_2 was first proposed as 0.9. Here, \circ denotes the per-coordinate multiplication. Then, RMSprop updates as:

$$\theta_{t+1,i} = \theta_{t,i} - \frac{\eta}{\sqrt{\mathcal{E}_{t+1,i}^{g \circ g} + \varepsilon}} \cdot g_{t,i}, \quad \forall t.$$

where momentum can be optionally added. Finally, Adam [17] adds an exponentially decaying average of past gradients: $\mathcal{E}_{t+1}^g = \beta_1 \cdot \mathcal{E}_t^g + (1 - \beta_1) \cdot g_t$, leading to the recursion:¹

$$\theta_{t+1,i} = \theta_{t,i} - \frac{\eta}{\sqrt{\mathcal{E}_{t+1,i}^{g \circ g} + \varepsilon}} \cdot \mathcal{E}_{t+1,i}^g, \quad \forall t,$$

where usually $\beta_1 = 0.9$ and $\beta_2 = 0.999$. Adam is equivalent to RMSprop when $\beta_1 = 0$ and no bias correction is applied.

3 DEMON: Decaying momentum algorithm

Algorithm 1 DEMON in SGDM

Parameters: # of iterations T , step size η , momentum initial value β_{init} .
 $v_t = \theta_t = 0$, otherwise randomly initialized.
for $t = 0, \dots, T$ **do**

$$\beta_t = \beta_{\text{init}} \cdot \frac{\left(1 - \frac{t}{T}\right)}{\left(1 - \beta_{\text{init}}\right) + \beta_{\text{init}} \left(1 - \frac{t}{T}\right)}$$

$$\theta_{t+1} = \theta_t - \eta g_t + \beta_t v_t$$

$$v_{t+1} = \beta_t v_t - \eta g_t$$

end for

Algorithm 2 DEMON in Adam

Parameters: # of iterations T , step size η , momentum initial value β_{init} , $\beta_2, \varepsilon = 10^{-8}$.
 $v_t = \theta_t = \mathcal{E}_0^{g \circ g} = 0$, otherwise randomly initialized.
for $t = 0, \dots, T$ **do**

$$\beta_t = \beta_{\text{init}} \cdot \frac{\left(1 - \frac{t}{T}\right)}{\left(1 - \beta_{\text{init}}\right) + \beta_{\text{init}} \left(1 - \frac{t}{T}\right)}$$

$$\mathcal{E}_{t+1}^{g \circ g} = \beta_2 \cdot \mathcal{E}_t^{g \circ g} + (1 - \beta_2) \cdot (g_t \circ g_t)$$

$$m_{t,i} = g_{t,i} + \beta_t m_{t-1,i}$$

$$\theta_{t+1,i} = \theta_{t,i} - \frac{\eta}{\sqrt{\mathcal{E}_{t+1,i}^{g \circ g} + \varepsilon}} \cdot m_{t,i}$$

end for

Motivation and interpretation. DEMON is motivated by linear learning rate decay models which reduce the impact of a gradient to current and future updates. By decaying the momentum parameter, we decay the total contribution of a gradient to all future updates. *Our goal here is to present a concrete, effective, and easy-to-use momentum decay procedure which we show in the experimental section.* By Occam’s Razor, a linear decay achieves such a goal since it is simple and requires no tuning in most cases. The key component is the momentum decay schedule:

$$\beta_t = \beta_{\text{init}} \cdot \frac{\left(1 - \frac{t}{T}\right)}{\left(1 - \beta_{\text{init}}\right) + \beta_{\text{init}} \left(1 - \frac{t}{T}\right)}. \quad (1)$$

Above, the fraction $(1 - t/T)$ refers to the proportion of iterations remaining. The interpretation of this rule comes from the following argument: Assume fixed momentum parameter $\beta_t \equiv \beta$; e.g., $\beta = 0.9$, as literature dictates. For our discussion, we will use the SGDM recursion. We know that $v_0 = 0$, and $v_t = \beta v_{t-1} - \eta g_t$. Then, the main recursion can be unrolled into:

$$\theta_{t+1} = \theta_t - \eta g_t - \eta \beta g_{t-1} - \eta \beta^2 g_{t-2} + \eta \beta^3 v_{t-2} = \dots = \theta_t - \eta g_t - \eta \cdot \sum_{i=1}^t (\beta^i \cdot g_{t-i})$$

Interpreting the above recursion, *a particular gradient term g_t contributes a total of $\eta \sum_i \beta^i$ of its “energy” to all future gradient updates.* Moreover, for an asymptotically large number of iterations, we know that β contributes on up to $t - 1$ terms. Then, $\sum_{i=1}^{\infty} \beta^i = \beta \sum_{i=0}^{\infty} \beta^i = \beta / (1 - \beta)$. Thus, in our quest for a decaying schedule and for a simple linear momentum decay, it is natural to consider a scheme where the cumulative momentum is decayed to 0. Let β_{init} be the initial β ; then at current step t with total T steps, we design the decay routine such that: $\beta / (1 - \beta) = (1 - t/T) \beta_{\text{init}} / (1 - \beta_{\text{init}})$. This leads to equation 1. Although β changes in subsequent iterations, this is typically a very close approximation since $\beta^i \beta^{i+1} \dots \beta^t$ for a particular g^i diminishes much faster than β changes.

Connection to previous algorithms. DEMON introduces an implicit discount factor. The main recursions of the algorithm are the same with standard algorithms in machine learning. E.g., for $\beta_t = \beta = 0.9$ we obtain SGD with momentum, and for $\beta = 0$ we obtain plain SGD in Algorithm 1; in Algorithm 2, for $\beta_1 = 0.9$ with a slightly adjustment of learning rate we obtain Adam, while for $\beta_1 = 0$ we obtain a non-accumulative AdaGrad algorithm. We choose to apply DEMON to a slightly adjusted Adam—instead of vanilla Adam—to isolate the effect of the momentum parameter, since the momentum parameter adjusts the magnitude of the current gradient as well in vanilla Adam.

Efficiency. DEMON requires only limited extra overhead and computation in comparison to the vanilla counterparts for the computation of β_t . Implementation is simply 1-2 lines of code.

¹For clarity, we will skip the bias correction step in this description of Adam; see [17].

$$\begin{aligned} p_t &= (\text{iters} - t) / \text{iters} \\ \text{beta}_t &= \text{beta}_1 * (p_t / (1 - \text{beta}_1 + \text{beta}_1 * p_t)) \end{aligned}$$

Convergence analysis. We provide a convergence proof for DEMON SGDM in the convex setting, and a convergence result for DEMON Adam in the non-convex setting. See Appendix B for details. Convergence analysis of a toy convex problem is given in Appendix C.

Practical suggestions. For settings in which β_{init} is typically large, such as image classification, we advocate for decaying momentum from β_{init} at $t = 0$, to 0 at $t = T$ as a general rule. We also observe and report improved performance by delaying momentum decay till later epochs. In many cases, performance can be further improved by decaying to a small negative value, such as -0.3.

4 Related work

Numerous techniques exist for automatic hyperparameter tuning. Learning rate adaptive methods, such as AdaGrad [14], AdaDelta [15], RMSprop [16], and Adam [17], are most widely used. Adam, the most popular, combines a momentum term with the current gradient before multiplying with an adaptive learning rate. Interest in closing the generalization difference between adaptive methods and SGDM led to AMSGrad [25], which uses the maximum of the exponential moving average of squared gradients, QHAdam [18], a variant of QHM that recovers a variety of optimization algorithms, AdamW [39], which decouples weight decay in Adam, and Padam [40], which lowers the exponent of the second moment.

Asynchronous methods are commonly used in deep learning, and [27] show that running SGD asynchronously is similar to adding a momentum-like term to SGD without assumptions of convexity of the objective function. They demonstrate this natural connection empirically on CNNs. This implies that the momentum parameter needs to be tuned according to the level of asynchrony. YellowFin [28] is a learning rate and momentum adaptive method for both the synchronous and asynchronous setting motivated by a quadratic model analysis and robustness insights. In the non-convex setting, STORM [41] uses a variant of momentum for variance reduction.

The convergence of momentum methods has been heavily explored both empirically and theoretically [42, 43, 44, 45]. [11] explored momentum schedules, even increasing momentum during training, inspired by Nesterov’s routines for convex optimization. [46] scales the batch size to create associated changes in learning rate and momentum. [47] introduces cycles of simultaneously increasing learning rate and decreasing momentum followed by simultaneously decreasing learning rate and increasing momentum. Some work adapts the momentum to reduce oscillations during training [48] and explores integration of momentum into well-conditioned convex problems [49]. Another approach is to combine several momentum vectors with different β values [50]. We are aware of the theoretical work of [51] that proves, under certain conditions, SGDM is equivalent to SGD with a rescaled learning rate, but our experiments in the deep learning setting show slightly different behavior. Understanding this discrepancy is an exciting direction of research.

Smaller values of β have gradually been employed for Generative Adversarial Networks (GANs), and recent developments in game dynamics [32] show a negative momentum is helpful.

5 Experiments

We separate experiments into those with adaptive learning rate and those with adaptive momentum, following [18]. All settings, with exact hyper-parameters, are briefly summarized in Table 1 and comprehensively detailed in Appendix A. We report improved performance by delaying the application of DEMON where applicable, and report performance across different number of total epochs to demonstrate effectiveness regardless of the training budget. Note the pre-defined number of epochs affects the proposed decaying momentum routine by definition of β_t .

5.1 Decreasing the need for hyperparameter tuning

In this section, we demonstrate the robustness of DEMON SGDM and DEMON Adam relative to SGDM with learning rate decay and Adam. A grid search is performed over learning rate and momentum. For SGDM, we apply the commonly used learning rate decay schedule in literature, decaying the learning rate by a factor of 0.1 at 50% and 75% of the total epochs. Generalization error under several hyperparameter settings is presented in Figure 1.

WRN-STL10-DEMONSGDM yields a significantly larger band of lighter color, indicating better performance for a wide range of hyperparameters. For every learning rate-momentum pair, we observe a lighter color for DEMON SGDM

Table 1: Summary of experimental settings.

Experiment short name	Model	Dataset	Optimizer
RN18-CIFAR10-DEMONGSDM	ResNet18	CIFAR10	DEMON SGDM
RN18-CIFAR10-DEMONAdam	ResNet18	CIFAR10	DEMON Adam
RN56-TINYIMAGENET-DEMONGSDM	ResNet56	Tiny ImageNet	DEMON SGDM
RN56-TINYIMAGENET-DEMONAdam	ResNet56	Tiny ImageNet	DEMON Adam
VGG16-CIFAR100-DEMONGSDM	VGG-16	CIFAR100	DEMON SGDM
VGG16-CIFAR100-DEMONAdam	VGG-16	CIFAR100	DEMON Adam
WRN-STL10-DEMONGSDM	Wide ResNet 16-8	STL10	DEMON SGDM
WRN-STL10-DEMONAdam	Wide ResNet 16-8	STL10	DEMON Adam
LSTM-PTB-DEMONGSDM	LSTM RNN	Penn TreeBank	DEMON SGDM
LSTM-PTB-DEMONAdam	LSTM RNN	Penn TreeBank	DEMON Adam
VAE-MNIST-DEMONGSDM	VAE	MNIST	DEMON SGDM
VAE-MNIST-DEMONAdam	VAE	MNIST	DEMON Adam
NCSN-CIFAR10-DEMONAdam	NCSN	CIFAR10	DEMON Adam
CAPS-FMNIST-DEMONAdam	Capsnet	FMNIST	DEMON Adam

relative to SGDM. Concretely, SGDM has roughly one configuration per column with less than 22% generalization error, while DEMON SGDM has five.

On VGG16-CIFAR100-DEMONGSDM, a larger band of low generalization error exists compared to SGDM. There also appears to be a slight shift in optimal parameters. Concretely, DEMON SGDM has almost three times the number of configurations with generalization error less than 31%.

On RN18-CIFAR10-DEMONAdam, DEMON Adam demonstrates its improved hyperparameter robustness. The generalization errors achieved with Adam fluctuate significantly, yielding optimal performance with only a few hyperparameter settings. In contrast, DEMON Adam yields a wide band of high performance across hyperparameters.

These results indicate that both DEMON Adam and SGDM are less sensitive to hyperparameter tuning than their vanilla counterparts, whilst providing the same or better performance. This is critical to the use of DEMON in practice, as DEMON can be used with no tuning. The results also suggest DEMON can further benefit from high momentum values.

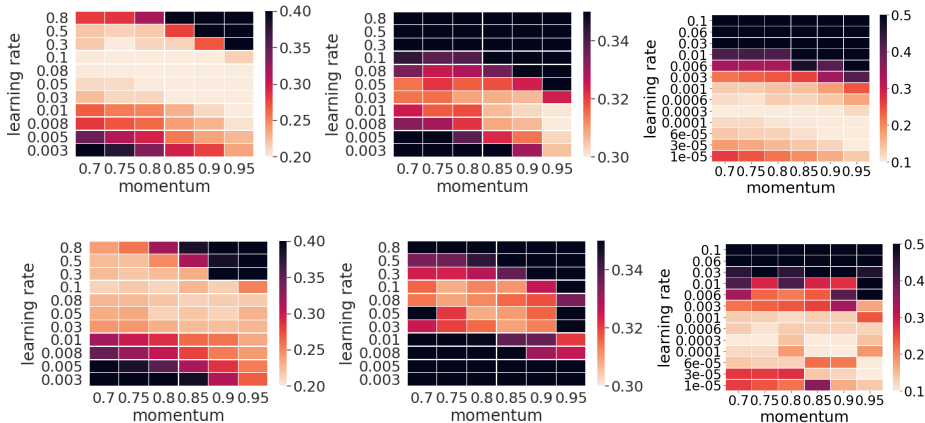


Figure 1: In order from left to right: Error rate for WRN-STL10-DEMONGSDM (top) and WRN-STL10-SGDM (bottom) for 50 epochs, error rate for VGG16-CIFAR100-DEMONGSDM (top) and VGG16-CIFAR100-SGDM (bottom) for 100 epochs, and error rate for RN18-CIFAR10-DEMONAdam and RN18-CIFAR10-Adam for 100 epochs. Light-colored patches indicate better performance.

5.2 Comparison of adaptive methods

DEMON Adam (Algorithm 2) is applied to a variety of models and tasks. We select Adam [17] as the baseline algorithm and include comparisons with state-of-the-art adaptive learning rate methods Quasi-Hyperbolic Adam (QHAdam) [18], AMSGrad [25], AdamW [39], YellowFin [28] (descriptions in Appendix A.2.1). We emphasize that Quasi-Hyperbolic methods are capable of recovering Accelerated SGD [52], Nesterov Accelerated Gradient [53], Synthesized Nesterov Variants [54], and others, thus covering more algorithms than those present. We tune all learning

Table 2: RN18-CIFAR10-DEMONSGDM/Adam and VGG16-CIFAR100-DEMONSGDM/Adam generalization error. The number of epochs was predefined before the execution of the algorithms.

	ResNet 18				VGG-16		
	30 epochs	75 epochs	150 epochs	300 epochs	75 epochs	150 epochs	300 epochs
SGDM	11.80 ± .11	8.82 ± .25	8.43 ± .07	7.32 ± .14	35.04 ± .24	30.09 ± .32	27.83 ± .30
AggMo	11.14 ± .34	8.71 ± .24	7.93 ± .15	7.62 ± .03	34.40 ± .60	30.75 ± .55	28.64 ± .45
QHM	10.66 ± .17	8.72 ± .14	7.95 ± .17	7.67 ± .10	33.27 ± .56	29.93 ± .13	29.01 ± .54
Adam	16.58 ± .18	13.63 ± .22	11.90 ± .06	11.94 ± .06	37.98 ± .20	33.62 ± .11	31.09 ± .09
AMSGrad	16.98 ± .36	13.43 ± .14	11.83 ± .12	10.48 ± .12	40.67 ± .65	34.46 ± .21	31.62 ± .12
AdamW	15.39 ± .46	12.46 ± .52	11.38 ± .21	10.50 ± .17	36.96 ± 1.21	33.48 ± .68	32.22 ± .13
QHAdam	16.41 ± .38	15.55 ± .25	13.78 ± .08	13.36 ± .11	36.53 ± .20	32.96 ± .11	30.97 ± .10
YellowFin	17.25 ± .15	13.66 ± .34	12.13 ± .41	11.39 ± .16	86.24 ± 3.54	68.87 ± 5.82	50.18 ± 4.02
DEMON SGDM	10.21 ± .15	8.45 ± .28	7.82 ± .27	7.30 ± .16	31.67 ± .49	28.86 ± .16	27.71 ± .05
DEMON Adam	11.75 ± .15	9.69 ± .10	8.83 ± .08	8.44 ± .05	32.40 ± .19	28.84 ± .18	27.11 ± .19

Table 3: WRN-STL10-DEMONSGDM/Adam generalization error, PTB-LSTM-DEMONSGDM/Adam generalization perplexity, and CAPS-FMNIST-DEMONSGDM/Adam generalization error. The number of epochs was predefined before the execution of the algorithms.

	Wide Residual 16-8			LSTM		Capsule Network	
	50 epochs	100 epochs	200 epochs	25 epochs	39 epochs	50 epochs	100 epochs
SGDM	22.42 ± .56	17.20 ± .35	14.51 ± .26	89.59 ± .07	87.57 ± .11	-	-
AggMo	21.37 ± .32	17.15 ± .35	14.49 ± .26	89.09 ± .16	89.07 ± .15	-	-
QHM	21.75 ± .31	18.21 ± .48	14.44 ± .23	94.47 ± .19	94.44 ± .13	-	-
Adam	23.35 ± .20	19.63 ± .26	18.65 ± .07	115.54 ± .64	115.02 ± .52	9.27 ± .08	9.25 ± .11
AMSGrad	21.73 ± .25	19.35 ± .20	18.21 ± .18	108.07 ± .19	107.87 ± .25	9.39 ± .18	9.28 ± .19
AdamW	20.39 ± .62	18.55 ± .23	17.00 ± .41	116.27 ± 2.57	116.21 ± 2.14	9.78 ± 0.62	9.92 ± .74
QHAdam	21.25 ± .22	19.81 ± .18	18.52 ± .25	112.52 ± .23	112.45 ± .39	9.30 ± .23	9.24 ± .15
YellowFin	22.55 ± .14	20.68 ± .04	18.56 ± .33	123.52 ± .52	115.55 ± .23	10.96 ± .65	10.55 ± .84
DEMON SGDM	19.45 ± .20	15.98 ± .40	13.67 ± .13	88.33 ± .16	88.32 ± .12	-	-
DEMON Adam	19.42 ± .10	17.82 ± .34	16.87 ± .36	101.57 ± .32	101.44 ± .47	8.82 ± .12	8.76 ± .13

rates in rough multiples of 3 and keep all other parameters close to those recommended in the original literature. For DEMON Adam, we set $\beta_{\text{init}} = 0.9$, $\beta_2 = 0.999$ and decay from β_{init} to 0 in all experiments.

To simplify the presentation of results, further comparison against Padam [40] and the OneCycle routine [47] can be found in Appendix F. DEMON outperforms both approaches in various settings.

Residual Network (RN18-CIFAR10-DEMONAdam). We train a ResNet18 [2] model on the CIFAR-10 dataset. With DEMON Adam, we achieve the generalization error reported in the literature [2], attained using SGDM and a curated learning rate decay schedule, while all other adaptive methods are not competitive (see Table 2). DEMON Adam continues learning after other methods have plateaued, outperforming other adaptive methods by a 2%-5% generalization error across all experiments (see Appendix E Figure 5).

(RN56-TINYIMAGENET-DEMONAdam). We train a ResNet56 [2] model on the Tiny ImageNet dataset. Using DEMON Adam, we achieve superior generalization performance over Adam, which was found to be quite sensitive to hyperparameter settings. DEMON Adam outperformed Adam on Tiny ImageNet by a 8%-12% margin in generalization error (see Table 4).

Non-Residual Network (VGG16-CIFAR100-DEMONAdam). We train an adjusted VGG-16 model [33] on the CIFAR-100 dataset. Again, DEMON Adam continues to improve after other methods begin to plateau. This behavior results in a 1-3% decrease in generalization error compared to reported results with the same model and task [55], attained with SGDM and a curated learning rate decay schedule. DEMON Adam achieves a 3%-6% generalization error improvement over all other methods (see Appendix E Figure 5 and Table 2).

Wide Residual Network (WRN-STL10-DEMONAdam). We train a Wide Residual 16-8 model [21] on the STL-10 dataset, which has significantly fewer, higher resolution images in comparison to the CIFAR datasets. In this setting, DEMON Adam significantly outperforms other methods in the latter stages of training. DEMON Adam achieves a 0.5%-2% generalization error margin over other methods with a small and large number of epochs (see Appendix E Figure 5 and Table 3).

Capsule Network (CAPS-FMNIST-DEMONAdam). Capsule Networks [36] represent Neural Networks as a set of capsules that each encode a specific entity or meaning. Capsules exploit the observation that viewpoint changes significantly alter pixels but are linear with respect to the pose matrix. The activation of capsules differs from standard neural

Table 4: RN56-TINYIMAGENET-DEMONGSDM/Adam generalization error, VAE-MNIST-DEMONGSDM/Adam generalization loss, and NCSN-CIFAR10-DEMONGSDM inception score. The number of epochs was predefined before the execution of the algorithms.

	Resnet 56			VAE		NCSN
	20 epochs	40 epochs	50 epochs	100 epochs	200 epochs	512 epochs
SGDM	45.98 ± .21	41.66 ± .10	140.28 ± .51	137.70 ± .93	136.34 ± .31	-
AggMo	-	-	139.49 ± .99	136.56 ± .28	134.93 ± .40	-
QHM	-	-	142.47 ± .50	137.97 ± .54	135.97 ± .29	-
Adam	57.56 ± 1.50	50.89 ± .59	136.28 ± .18	134.64 ± .14	134.66 ± .17	8.15 ± .20
AMSGrad	-	-	137.89 ± .12	135.69 ± .03	134.75 ± .18	-
QHAdam	-	-	136.69 ± .17	134.84 ± .08	134.12 ± .12	-
YellowFin	-	-	414.74 ± 5.00	351.80 ± 6.68	286.69 ± 6.68	-
DEMON SGDM	44.55 ± .32	41.64 ± .16	136.50 ± .56	135.30 ± .93	-	-
DEMON Adam	45.96 ± .32	41.80 ± .21	134.46 ± .17	134.12 ± .08	133.87 ± .21	8.07 ± .08

network activation functions because it depends on comparing incoming pose predictions. We train Capsule Networks on the FMNIST dataset and show that DEMON Adam outperforms other methods (see Table 3).

LSTM (PTB-LSTM-DEMONGSDM). We apply an LSTM [34] to the language modeling task, which can have sharp gradient distributions (e.g., rare words). While all other adaptive methods overfit to this task, DEMON Adam achieves a margin of 6-14 in generalization perplexity (see Appendix E Figure 5 and Table 3).

Variational AutoEncoder (VAE-MNIST-DEMONGSDM). Generative modeling is a branch of unsupervised learning that focuses on learning the underlying data distribution. VAEs [35] are generative models that pair a generator network with a recognition model that performs approximate inference and can be trained with backpropagation. We train VAEs on the MNIST dataset. DEMON Adam outperforms all other methods, particularly with fewer epochs (see Table 4, Appendix E Figure 5).

Noise Conditional Score Network (NCSN-CIFAR10-DEMONGSDM). NCSN [37] is a recent generative model that estimates gradients of the data distribution with score matching and produces samples via Langevin dynamics with these gradients. We train a NCSN on the CIFAR10 dataset, for which NCSN achieves state-of-the-art inception score. Although Adam achieves a superior inception score (see Table 4), the results seen in Figure 2 exhibit a noticeably unnatural green compared to those produced by DEMON Adam.



Figure 2: Randomly selected CIFAR10 images generated with NCSN. Left: Real CIFAR10 images. Middle: Adam. Right: DEMON Adam.

5.3 Non-adaptive momentum methods

We apply DEMON SGDM (Algorithm 1) to a variety of models and tasks. SGDM with learning rate decay is used as a baseline because it often achieves state-of-the-art results for such tasks. Experiments with recent adaptive momentum methods Aggregated Momentum (AggMo) [50] and Quasi-Hyperbolic Momentum (QHM) [18] are included (descriptions in Appendix A.2.2). We exclude accelerated SGD [52] due to tuning difficulties. We again tune all learning rates in rough multiples of 3 and keep other parameters close to values recommended in the literature. For SGDM, AggMo, and QHM, we decay the learning rate at 50% and 75% of total epochs by a factor of 0.1, except for the PTB-LSTM-DEMONGSDM setting. For DEMON SGDM, we apply no learning rate decay, set $\beta_{\text{init}} = 0.9$ for most experiments, and generally decay from β_{init} to 0.

We emphasize that DEMON can be combined with any momentum method. We present DEMON SGDM since SGDM is the most widely used optimizer.

Residual Network (RN18-CIFAR10-DEMONGSDM). We train a ResNet18 model on the CIFAR-10 dataset. With DEMON SGDM, we achieve better generalization error than SGDM. Additionally, DEMON SGDM outperforms other adaptive momentum methods with learning rate decay schedules (see Table 2), demonstrating the strong performance of DEMON relative to learning rate decay.

(RN56-TINYIMAGENET-DEMONGSDM). We train a ResNet56 model on the Tiny ImageNet dataset. DEMON SGDM outperforms SGDM with learning rate decay when fewer epochs are used and matches performance when more epochs are used (see Table 4). The performance achieved with SGDM was found to be sensitive to hyperparameter settings, while DEMON SGDM performed comparably for a wide range of hyperparameters.

Non-Residual Network (VGG16-CIFAR100-DEMONGSDM). We train an adjusted VGG-16 model on the CIFAR-100 dataset. DEMON SGDM learns slowly in initial epochs but continues to learn after the performance of other methods plateaus, yielding superior final performance. DEMON SGDM improves on all other methods in generalization error margin (see Table 2).

Wide Residual Network (WRN-STL10-DEMONGSDM). We train a Wide Residual 16-8 model on the STL-10 dataset. DEMON SGDM outperforms all other methods by a 1%-2% generalization error margin with a small and large number of epochs (see Table 3).

LSTM (PTB-LSTM-DEMONGSDM). We train an LSTM architecture for the PTB language modeling task. DEMON SGDM slightly outperforms other adaptive momentum methods in generalization perplexity and is competitive with SGDM (see Table 3).

Variational AutoEncoder (VAE-MNIST-DEMONGSDM). We train a generative VAE model on the MNIST dataset. DEMON SGDM outperforms all other methods in terms of generalization loss for fewer epochs and is competitive when more epochs are used (see Table 4).

6 Additional Experimental Results

Additional experimental results are given in the Appendix and we provide summaries in this section. In Appendix F, we demonstrate superior performance of DEMON SGDM over Padam [40] and OneCycle [47] on RN18-CIFAR10-DEMONGSDM, VGG16-CIFAR100-DEMONGSDM and VAE-MNIST-DEMONGSDM settings. In Appendix D, we demonstrate the superior performance DEMON SGDM over an effective learning rate adjusted SGD. In Appendix A.3, we run all experiments from Section 5.3 without learning rate decay. On RN18-CIFAR10-DEMONGSDM, DEMON SGDM outperforms all other adaptive momentum methods by a 3%-8% validation error margin with a small and large number of epochs. On VGG16-CIFAR100-DEMONGSDM, DEMON SGDM achieves a 1%-8% improvement in generalization error over all other methods. Similarly, there exists a clear margin of improvement in the performance of DEMON SGDM for all settings that were tested.

7 Conclusion

We show the effectiveness of the proposed momentum decay rule, DEMON, across a number of datasets and architectures. The adaptive optimizer Adam combined with DEMON is empirically substantially superior to the popular Adam, in addition to other state-of-the-art adaptive learning rate algorithms, suggesting a drop-in replacement. It is also demonstrated that DEMON SGDM generally improves on SGDM with learning rate decay schedule, as well as other state-of-the-art adaptive momentum methods. Furthermore, DEMON is shown to significantly improve hyperparameter robustness. DEMON is computationally cheap, understandable, and easy to implement. We hope it is useful in practice and as a subject of future research.

References

- [1] Alex Krizhevsky, Ilya Sutskever, and Geoffrey E Hinton. Imagenet classification with deep convolutional neural networks. In *Advances in neural information processing systems*, pages 1097–1105, 2012.
- [2] Kaiming He, Xiangyu Zhang, Shaoqing Ren, and Jian Sun. Deep residual learning for image recognition. In *Proceedings of the IEEE conference on computer vision and pattern recognition*, pages 770–778, 2016.
- [3] Shaoqing Ren, Kaiming He, Ross Girshick, and Jian Sun. Faster R-CNN: Towards real-time object detection with region proposal networks. In *Advances in neural information processing systems*, pages 91–99, 2015.
- [4] Tomas Mikolov, Ilya Sutskever, Kai Chen, Greg S Corrado, and Jeff Dean. Distributed representations of words and phrases and their compositionality. In *Advances in neural information processing systems*, pages 3111–3119, 2013.
- [5] Dzmitry Bahdanau, Kyunghyun Cho, and Yoshua Bengio. Neural machine translation by jointly learning to align and translate. *arXiv preprint arXiv:1409.0473*, 2014.

- [6] Jonas Gehring, Michael Auli, David Grangier, Denis Yarats, and Yann N Dauphin. Convolutional sequence to sequence learning. In *Proceedings of the 34th International Conference on Machine Learning-Volume 70*, pages 1243–1252. JMLR. org, 2017.
- [7] Haşim Sak, Andrew Senior, and Françoise Beaufays. Long short-term memory recurrent neural network architectures for large scale acoustic modeling. In *Fifteenth annual conference of the international speech communication association*, 2014.
- [8] Tom Sercu, Christian Puhersch, Brian Kingsbury, and Yann LeCun. Very deep multilingual convolutional neural networks for LVCSR. In *2016 IEEE International Conference on Acoustics, Speech and Signal Processing (ICASSP)*, pages 4955–4959. IEEE, 2016.
- [9] Tom Brown, Benjamin Mann, Nick Ryder, Melanie Subbiah, Jared Kaplan, Prafulla Dhariwal, Arvind Neelakantan, Pranav Shyam, Girish Sastry, Amanda Askell, Sandhini Agarwal, Ariel Herbert-Voss, Gretchen Krueger, Tom Henighan, Rewon Child, Aditya Ramesh, Daniel Ziegler, Jeffrey Wu, Clemens Winter, Christopher Hesse, Mark Chen, Eric Sigler, Mateusz Litwin, Scott Gray, Benjamin Chess, Jack Clark, Christopher Berner, Sam McCandlish, Alec Radford, Ilya Sutskever, and Dario Amodei. Language models are few-shot learners. *arXiv preprint arXiv:2005.14165*, 2020.
- [10] Or Sharir, Barak Peleg, and Yoav Shoham. The cost of training nlp models: A concise overview. *arXiv preprint arXiv:2004.08900*, 2020.
- [11] Ilya Sutskever, James Martens, George Dahl, and Geoffrey Hinton. On the importance of initialization and momentum in deep learning. In *International conference on machine learning*, pages 1139–1147, 2013.
- [12] Ian Goodfellow, Yoshua Bengio, Aaron Courville, and Yoshua Bengio. *Deep learning*, volume 1. MIT Press, 2016.
- [13] Ashia C Wilson, Rebecca Roelofs, Mitchell Stern, Nati Srebro, and Benjamin Recht. The marginal value of adaptive gradient methods in machine learning. In *Advances in Neural Information Processing Systems*, pages 4148–4158, 2017.
- [14] John Duchi, Elad Hazan, and Yoram Singer. Adaptive subgradient methods for online learning and stochastic optimization. *Journal of Machine Learning Research*, 12(Jul):2121–2159, 2011.
- [15] Matthew D Zeiler. Adadelta: an adaptive learning rate method. *arXiv preprint arXiv:1212.5701*, 2012.
- [16] Geoffrey Hinton, Nitish Srivastava, and Kevin Swersky. Neural networks for machine learning lecture 6a overview of mini-batch gradient descent. *Cited on*, 14:8, 2012.
- [17] Diederik P Kingma and Jimmy Ba. Adam: A method for stochastic optimization. *arXiv preprint arXiv:1412.6980*, 2014.
- [18] Jerry Ma and Denis Yarats. Quasi-hyperbolic momentum and Adam for deep learning. *arXiv preprint arXiv:1810.06801*, 2018.
- [19] Vatsal Shah, Anastasios Kyrillidis, and Sujay Sanghavi. Minimum norm solutions do not always generalize well for over-parameterized problems. *arXiv preprint arXiv:1811.07055*, 2018.
- [20] Saining Xie, Ross Girshick, Piotr Dollár, Zhuowen Tu, and Kaiming He. Aggregated residual transformations for deep neural networks. In *Proceedings of the IEEE conference on computer vision and pattern recognition*, pages 1492–1500, 2017.
- [21] Sergey Zagoruyko and Nikos Komodakis. Wide residual networks. *arXiv preprint arXiv:1605.07146*, 2016.
- [22] Gao Huang, Zhuang Liu, Laurens Van Der Maaten, and Kilian Q Weinberger. Densely connected convolutional networks. In *Proceedings of the IEEE conference on computer vision and pattern recognition*, pages 4700–4708, 2017.
- [23] Andrew G Howard, Menglong Zhu, Bo Chen, Dmitry Kalenichenko, Weijun Wang, Tobias Weyand, Marco Andreetto, and Hartwig Adam. Mobilenets: Efficient convolutional neural networks for mobile vision applications. *arXiv preprint arXiv:1704.04861*, 2017.
- [24] Jianmin Chen, Xinghao Pan, Rajat Monga, Samy Bengio, and Rafal Jozefowicz. Revisiting distributed synchronous SGD. *arXiv preprint arXiv:1604.00981*, 2016.
- [25] Sashank J Reddi, Satyen Kale, and Sanjiv Kumar. On the convergence of Adam and beyond. *arXiv preprint arXiv:1904.09237*, 2019.
- [26] Adam Paszke, Sam Gross, Soumith Chintala, Gregory Chanan, Edward Yang, Zachary DeVito, Zeming Lin, Alban Desmaison, Luca Antiga, and Adam Lerer. Automatic differentiation in pytorch. 2017.

- [27] Ioannis Mitliagkas, Ce Zhang, Stefan Hadjis, and Christopher Ré. Asynchrony begets momentum, with an application to deep learning. In *2016 54th Annual Allerton Conference on Communication, Control, and Computing (Allerton)*, pages 997–1004. IEEE, 2016.
- [28] Jian Zhang and Ioannis Mitliagkas. Yellowfin and the art of momentum tuning. *arXiv preprint arXiv:1706.03471*, 2017.
- [29] Mehdi Mirza and Simon Osindero. Conditional generative adversarial nets. *arXiv preprint arXiv:1411.1784*, 2014.
- [30] Alec Radford, Luke Metz, and Soumith Chintala. Unsupervised representation learning with deep convolutional generative adversarial networks. *arXiv preprint arXiv:1511.06434*, 2015.
- [31] Martin Arjovsky, Soumith Chintala, and Léon Bottou. Wasserstein GAN. *arXiv preprint arXiv:1701.07875*, 2017.
- [32] Gauthier Gidel, Reyhane Askari Hemmat, Mohammad Pezeshki, Remi Lepriol, Gabriel Huang, Simon Lacoste-Julien, and Ioannis Mitliagkas. Negative momentum for improved game dynamics. *arXiv preprint arXiv:1807.04740*, 2018.
- [33] Karen Simonyan and Andrew Zisserman. Very deep convolutional networks for large-scale image recognition. *arXiv preprint arXiv:1409.1556*, 2014.
- [34] Sepp Hochreiter and Jürgen Schmidhuber. Long short-term memory. *Neural computation*, 9(8):1735–1780, 1997.
- [35] Diederik P Kingma and Max Welling. Auto-encoding variational bayes. *arXiv preprint arXiv:1312.6114*, 2015.
- [36] Sara Sabour, Nicholas Fross, and Geoffrey Hinton. Dynamic routing between capsules. In *Advances in neural information processing systems*, 2017.
- [37] Yang Song and Stefano Ermon. Generative modeling by estimating gradients of the data distribution. *arXiv preprint arXiv:1907.05600*, 2019.
- [38] Sebastian Ruder. An overview of gradient descent optimization algorithms. *arXiv preprint arXiv:1609.04747*, 2016.
- [39] Ilya Loshchilov and Frank Hutter. Fixing weight decay regularization in adam. *arXiv preprint arXiv:1711.05101*, 2017.
- [40] Jinghui Chen and Quanquan Gu. Closing the generalization gap of adaptive gradient methods in training deep neural networks. *arXiv preprint arXiv:1806.06763*, 2018.
- [41] Ashok Cutkosky and Francesco Orabona. Momentum-based variance reduction in non-convex sgd. *arXiv preprint arXiv:1905.10018*, 2019.
- [42] Andre Wibisono and Ashia C Wilson. On accelerated methods in optimization. *arXiv preprint arXiv:1509.03616*, 2015.
- [43] Andre Wibisono, Ashia C Wilson, and Michael I Jordan. A variational perspective on accelerated methods in optimization. *proceedings of the National Academy of Sciences*, 113(47):E7351–E7358, 2016.
- [44] Ashia C Wilson, Benjamin Recht, and Michael I Jordan. A Lyapunov analysis of momentum methods in optimization. *arXiv preprint arXiv:1611.02635*, 2016.
- [45] Rahul Kidambi, Praneeth Netrapalli, Prateek Jain, and Sham Kakade. On the insufficiency of existing momentum schemes for stochastic optimization. In *2018 Information Theory and Applications Workshop (ITA)*, pages 1–9. IEEE, 2018.
- [46] Samuel Smith, Pieter-Jan Kindermans, Chris Ying, and Quoc Le. Don’t decay the learning rate, increase the batch size. *arXiv preprint arXiv:1711.00489*, 2017.
- [47] Leslie Smith. A disciplined approach to neural network hyper-parameters: Part 1 – learning rate, batch size, momentum, and weight decay. *arXiv preprint arXiv:1803.09820*, 2018.
- [48] Brendan Odonoghue and Emmanuel Candes. Adaptive restart for accelerated gradient schemes. *Foundations of computational mathematics*, 15(3):715–732, 2015.
- [49] Vishwak Srinivasan, Adepu Ravi Sankar, and Vineeth N Balasubramanian. Adine: an adaptive momentum method for stochastic gradient descent. In *Proceedings of the ACM India Joint International Conference on Data Science and Management of Data*, pages 249–256. ACM, 2018.
- [50] James Lucas, Shengyang Sun, Richard Zemel, and Roger Grosse. Aggregated momentum: Stability through passive damping. *arXiv preprint arXiv:1804.00325*, 2018.

- [51] Yuan. On the influence of momentum acceleration on online learning. *Journal of Machine Learning Research*, 17(192):1–66, 2016.
- [52] Prateek Jain, Sham M. Kakade, Rahul Kidambi, Praneeth Netrapalli, and Aaron Sidford. Accelerating stochastic gradient descent for least squares regression. *arXiv preprint arXiv:1704.08227*, 2017.
- [53] Yurii Nesterov. A method for solving the convex programming problem with convergence rate of $(1/k^2)$. *Soviet Mathematics Doklady*, 27(2):372–376, 1983.
- [54] Laurent Lessard, Benjamin Recht, and Andrew Packard. Analysis and design of optimization algorithms via integral quadratic constraints. *SIAM Journal on Optimization*, 26(1):57–95, 2016.
- [55] Swami Sankaranarayanan, Arpit Jain, Rama Chellappa, and Ser Nam Lim. Regularizing deep networks using efficient layerwise adversarial training. *arXiv preprint arXiv:1705.07819*, 2018.
- [56] Timothy Dozat. Incorporating nesterov momentum into adam. *ICLR Workshop, (1):20132016*, 2016.
- [57] Euhanna Ghadimi, Hamid Reza Feyzmahdavian, and Mikael Johansson. Global convergence of the heavyball method for convex optimization. *arXiv preprint arXiv:1412.7457*, 2014.
- [58] Fangyu Zou, Li Shen, Zequn Jie, Weizhong Zhang, and Wei Liu. A sufficient condition for convergences of adam and rmsprop. *arxiv preprint arXiv:1811.09358*, 2018.

A Experiments

We evaluated the momentum decay rule with Adam and SGDM on Residual CNNs, Non Residual CNNs, RNNs, generative models, and Capsule Networks. For CNNs, we used the image classification datasets CIFAR10, CIFAR100 and STL10 datasets. For RNNs, we used the language modeling dataset PTB. For generative modeling, we used the MNIST and CIFAR10 datasets. For Capsule Networks, we used FMNIST. For each network dataset pair other than NSCN and Capsule Networks, we evaluated Adam, QHAdam, AMSGrad, AdamW, YellowFin, DEMON Adam, AggMo, QHM, DEMON SGDM, SGDM. For adaptive learning rate methods and adaptive momentum methods, we generally perform a grid search over the learning rate. For SGDM, we generally perform a grid search over learning rate and initial momentum. For SGDM, Aggmo, and QHM, we decay the learning rate by 0.1 at 50% and 75% of the total epochs, following the standard in the literature.

A.1 Setup

We describe the eight test problems in this paper.

- **CIFAR10 - ResNet18** CIFAR10 contains 60,000 32x32x3 images with a 50,000 training set, 10,000 test set split. There are 10 classes. ResNet18 [2] is an 18 layers deep CNN with skip connections for image classification. Trained with a batch size of 128.
- **TINY IMAGENET - ResNet56** Tiny ImageNet contains 110,000 64x64x3 images with a 100,000 training set, 10,000 test set split. There are 200 classes. ResNet56 [2] is a 56 layer deep CNN with skip connections for image classification. Trained with a batch size of 128.
- **CIFAR100 - VGG16** CIFAR100 is a fine-grained version of CIFAR-10 and contains 60,000 32x32x3 images with a 50,000 training set, 10,000 test set split. There are 100 classes. VGG16 [33] is a 16 layers deep CNN with extensive use of 3x3 convolutional filters. Trained with a batch size of 128
- **STL10 - Wide ResNet 16-8** STL10 contains 1300 96x96x3 images with a 500 training set, 800 test set split. There are 10 classes. Wide ResNet 16-8 [21] is a 16 layers deep ResNet which is 8 times wider. Trained with a batch size of 64.
- **PTB - LSTM** PTB is an English text corpus containing 929,000 training words, 73,000 validation words, and 82,000 test words. There are 10,000 words in the vocabulary. The model is stacked LSTMs [34] with 2 layers, 650 units per layer, and dropout of 0.5. Trained with a batch size of 20.
- **FMNIST - CAPS MNIST** contains 60,000 32x32x1 grayscale images with a 50,000 training set, 10,000 test set split. There are 10 classes of 10 clothing items. Capsule Networks [36] represent Neural Networks as a set of capsules, where each capsule encodes a specific entity or meaning. The activations of capsules depend on comparing incoming pose predictions, as opposed to standard neural networks. The Capsule Network uses 3 iterations in the routing algorithm. Trained with a batch size of 128.
- **MNIST - VAE MNIST** contains 60,000 32x32x1 grayscale images with a 50,000 training set, 10,000 test set split. There are 10 classes of 10 digits. VAE [35] with three dense encoding layers and three dense decoding layers with a latent space of size 2. Trained with a batch size of 100.
- **CIFAR10 - NCSN** CIFAR10 contains 60,000 32x32x3 images with a 50,000 training set, 10,000 test set split. There are 10 classes. NCSN [37] is a recent state-of-the-art generative model which achieves the best reported inception score. We compute inception scores based on a total of 50000 samples. Since DEMON depends on a predefined number of epochs, we evaluate inception score at the end of training; otherwise, we follow the exact implementation in and defer details to the original paper.

A.2 Methods

A.2.1 Adaptive learning rate

Adam [17], as previously introduced in section 2, keeps an exponentially decaying average of squares of past gradients to adapt the learning rate. It also introduces an exponentially decaying average of gradients.

The Adam algorithm is parameterized by learning rate $\eta > 0$, discount factors $\beta_1 < 1$ and $\beta_2 < 1$, a small constant ϵ , and uses the update rule:

$$\begin{aligned}\mathcal{E}_{t+1}^g &= \beta_1 \cdot \mathcal{E}_t^g + (1 - \beta_1) \cdot g_t, \\ \mathcal{E}_{t+1}^{g \circ g} &= \beta_2 \cdot \mathcal{E}_t^{g \circ g} + (1 - \beta_2) \cdot (g_t \circ g_t), \\ \theta_{t+1,i} &= \theta_{t,i} - \frac{\eta}{\sqrt{\mathcal{E}_{t+1,i}^{g \circ g} + \epsilon}} \cdot \mathcal{E}_{t+1,i}^g, \quad \forall t.\end{aligned}$$

AMSGrad [25] resolves an issue in the proof of Adam related to the exponential moving average $\mathcal{E}_t^{g \circ g}$, where Adam does not converge for a simple optimization problem. Instead of an exponential moving average, AMSGrad keeps a running maximum of $\mathcal{E}^{g \circ g}$.

The AMSGrad algorithm is parameterized by learning rate $\eta > 0$, discount factors $\beta_1 < 1$ and $\beta_2 < 1$, a small constant ϵ , and uses the update rule:

$$\begin{aligned}\mathcal{E}_{t+1}^g &= \beta_1 \cdot \mathcal{E}_t^g + (1 - \beta_1) \cdot g_t, \\ \mathcal{E}_{t+1}^{g \circ g} &= \beta_2 \cdot \mathcal{E}_t^{g \circ g} + (1 - \beta_2) \cdot (g_t \circ g_t), \\ \hat{\mathcal{E}}_{t+1,i}^{g \circ g} &= \max(\hat{\mathcal{E}}_{t,i}^{g \circ g}, \mathcal{E}_{t,i}^{g \circ g}), \\ \theta_{t+1,i} &= \theta_{t,i} - \frac{\eta}{\sqrt{\hat{\mathcal{E}}_{t+1,i}^{g \circ g} + \epsilon}} \cdot \mathcal{E}_{t+1,i}^g, \quad \forall t,\end{aligned}$$

where \mathcal{E}_{t+1}^g and $\mathcal{E}_{t+1}^{g \circ g}$ are defined identically to Adam.

AdamW [39] modifies the typical implementation of weight decay regularization in Adam, by decoupling the weight decay from the gradient update. In particular, L2 regularization in Adam is usually implemented with the below modification where w_t is the rate of the weight decay at time t :

$$g_t = \nabla f(\theta_t) + w_t \theta_t,$$

while AdamW, instead, adjusts the weight decay term to appear in the gradient update:

$$\theta_{t+1,i} = \theta_{t,i} - \eta \left(\frac{1}{\sqrt{\mathcal{E}_{t+1,i}^{g \circ g} + \epsilon}} \cdot \mathcal{E}_{t+1,i}^g + w_{t,i} \theta_{t,i} \right), \quad \forall t.$$

QHAdam (Quasi-Hyperbolic Adam) [18] extends QHM (Quasi-Hyperbolic Momentum), introduced further below, to replace both momentum estimators in Adam with quasi-hyperbolic terms. This quasi-hyperbolic formulation is capable of recovering Adam and NAdam [56], amongst others.

The QHAdam algorithm is parameterized by learning rate $\eta > 0$, discount factors $\beta_1 < 1$ and $\beta_2 < 1$, $\nu_1, \nu_2 \in \mathbb{R}$, a small constant ϵ , and uses the update rule:

$$\begin{aligned}\mathcal{E}_{t+1}^g &= \beta_1 \cdot \mathcal{E}_t^g + (1 - \beta_1) \cdot g_t, \\ \mathcal{E}_{t+1}^{g \circ g} &= \beta_2 \cdot \mathcal{E}_t^{g \circ g} + (1 - \beta_2) \cdot (g_t \circ g_t), \\ \hat{\mathcal{E}}_{t+1}^g &= (1 + \beta_1^{t+1})^{-1} \cdot \mathcal{E}_{t+1}^g, \\ \hat{\mathcal{E}}_{t+1}^{g \circ g} &= (1 + \beta_2^{t+1})^{-1} \cdot \mathcal{E}_{t+1}^{g \circ g}, \\ \theta_{t+1,i} &= \theta_{t,i} - \eta \left[\frac{(1 - \nu_1) \cdot g_t + \nu_1 \cdot \hat{\mathcal{E}}_{t+1}^g}{\sqrt{(1 - \nu_2) g_t^2 + \nu_2 \cdot \hat{\mathcal{E}}_{t+1}^{g \circ g} + \epsilon}} \right], \quad \forall t,\end{aligned}$$

where \mathcal{E}_{t+1}^g and $\mathcal{E}_{t+1}^{g \circ g}$ are defined identically to Adam.

YellowFin [28] is motivated by robustness properties and analysis of quadratic objectives. For quadratic objectives, the optimizer tunes both the learning rate and the momentum to keep the hyperparameters within a region in which the convergence rate is a constant rate equal to the root momentum. This notion is extended empirically to non-convex objectives. On every iteration, YellowFin optimizes the hyperparameters to minimize a local quadratic optimization. Due to the many details, we defer an in-depth explanation to the paper [28].

A.2.2 Adaptive momentum

AggMo (Aggregated Momentum) [50] takes a linear combination of multiple momentum buffers. It maintains K momentum buffers, each with a different discount factor, and averages them for the update.

The AggMo algorithm is parameterized by learning rate $\eta > 0$, discount factors $\beta \in \mathbb{R}^K$, and uses the update rule:

$$(\mathcal{E}_{t+1}^g)^{(i)} = \beta^{(i)} \cdot (\mathcal{E}_t^g)^{(i)} + g_t, \quad \forall i \in [1, K],$$

$$\theta_{t+1,i} = \theta_{t,i} - \eta \left[\frac{1}{K} \cdot \sum_{i=1}^K (\mathcal{E}_{t+1}^g)^{(i)} \right], \quad \forall t.$$

QHM (Quasi-Hyperbolic Momentum) [18] is a weighted average of the momentum and plain SGD. QHM is capable of recovering Nesterov Momentum [53], Synthesized Nesterov Variants [54], accSGD [52] and others.

The QHM algorithm is parameterized by learning rate $\eta > 0$, discount factor $\beta < 1$, immediate discount factor $\nu \in \mathbb{R}$, and uses the update rule:

$$\mathcal{E}_{t+1}^g = \beta \cdot \mathcal{E}_t^g + (1 - \beta) \cdot g_t,$$

$$\theta_{t+1,i} = \theta_{t,i} - \eta \left[(1 - \nu) \cdot g_t + \nu \cdot \mathcal{E}_{t+1}^g \right], \quad \forall t.$$

A.3 Additional results for adaptive momentum methods

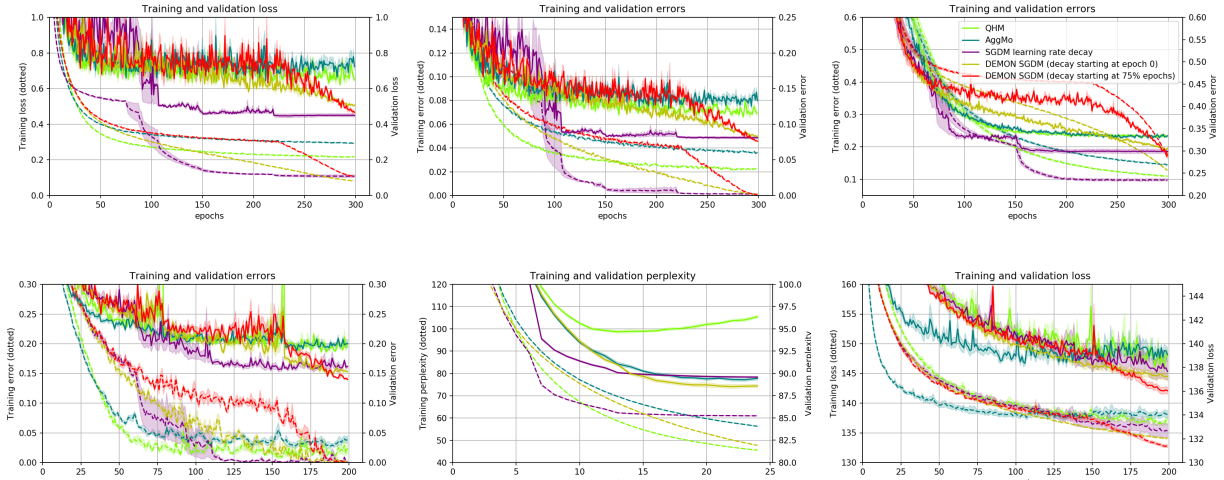


Figure 3: Top row, two left-most plot: RN18-CIFAR10-DEMONSGDM for 300 epochs. Top row, right-most plot: VGG16-CIFAR100-DEMONSGDM for 300 epochs. Bottom row, left-most plots: WRN-STL10-DEMONSGDM for 200 epochs. Bottom row, middle plot: PTB-LSTM-DEMONSGDM for 25 epochs. Bottom row, right-most plot: VAE-MNIST-DEMONSGDM for 200 epochs. Dotted and solid lines represent training and generalization metrics respectively. Shaded bands represent 1 standard deviation.

We present additional results for Aggregated Momentum (AggMo) [50], and Quasi-Hyperbolic Momentum (QHM) [18] without learning rate decay. Since SGDM with learning rate decay is most often used to achieve the state-of-the-art results with the architectures and tasks in question, we include SGDM with learning rate decay as the target to beat. SGDM with learning rate decay is implemented with a decay on validation error plateau, where we hand-tune the number of epochs to define plateau. We tune all learning rates in roughly multiples of 3 and try to keep all other parameters close to those recommended in the original literature. For DEMON SGDM, we leave $\beta_{\text{init}} = 0.9$ for most experiments and generally decay from β_{init} to 0.

Residual Neural Network (RN18-CIFAR10-DEMONSGDM). We train a ResNet18 model on the CIFAR-10 dataset. With DEMON SGDM, we achieve better generalization error than SGDM with learning rate decay, the optimizer for producing state-of-the-art results with ResNet architecture. The better performance of decaying momentum relative to learning rate decay is surprising.

	30 epochs	75 epochs	150 epochs	300 epochs
SGDM LR decay	11.29 ± .35	9.05 ± .07	8.26 ± .07	7.97 ± .14
AggMo	18.85 ± .27	13.02 ± .23	11.95 ± .15	10.94 ± .12
QHM	14.65 ± .24	12.66 ± .19	11.27 ± .13	10.42 ± .05
DEMON SGDM	10.39 ± .39	8.74 ± .28	7.82 ± .27	7.58 ± .04

Table 5: RN18-CIFAR10-DEMONGSDM generalization error with no learning rate decay. The number of epochs was predefined before the execution of the algorithms.

	VGG-16			Wide Residual 16-8		
	75 epochs	150 epochs	300 epochs	50 epochs	100 epochs	200 epochs
SGDM LR decay	35.29 ± .59	30.65 ± .31	29.74 ± .43	21.05 ± .27	17.83 ± 0.39	15.16 ± .36
AggMo	42.85 ± .89	34.25 ± .24	32.32 ± .18	22.70 ± .11	20.06 ± .31	17.90 ± .13
QHM	42.14 ± .79	33.87 ± .26	32.45 ± .13	22.86 ± .15	19.40 ± .23	17.79 ± .08
DEMON SGDM	33.08 ± .49	30.22 ± .50	28.99 (27.71) ± .16 (.05)	19.45 ± .20	15.98 ± .40	13.67 ± .13

Table 6: VGG16-CIFAR100-DEMONGSDM and WRN-STL10-DEMONGSDM generalization error with no learning rate decay. The number of epochs was predefined before the execution.

Running 5 seeds, DEMON SGDM outperforms all other adaptive momentum methods by a large 3%-8% validation error margin with a small and large number of epochs and is competitive or better than SGDM with learning rate decay. In Figure 3 (*Top row, two left-most plots*), DEMON SGDM is observed to continue learning after other adaptive momentum methods appear to begin to plateau.

Non-Residual Neural Network (VGG16-CIFAR100-DEMONGSDM). For the CIFAR-100 dataset, we train an adjusted VGG-16 model. In Figure 3 (*Top row, right-most plot*), we observe DEMON SGDM to learn slowly initially in loss and error, but similar to the previous setting it continues to learn after other methods begin to plateau, resulting in superior final generalization error.

Running 5 seeds, DEMON SGDM achieves an improvement of 1%-8% generalization error margin over all other methods. Refer to Table 6 for more details.

Wide Residual Neural Network (WRN-STL10-DEMONGSDM). We train a Wide Residual 16-8 model for the STL-10 dataset. In Figure 3 (*Bottom row, left-most plot*), training in both loss and error slows down quickly for other adaptive momentum methods with a large gap with SGDM learning rate decay. DEMON SGDM continues to improve and eventually catches up to SGDM learning rate decay.

Running 5 seeds, DEMON SGDM outperforms all other methods by a 1.5%-2% generalization error margin with a small and large number of epochs. Refer to Table 6 for more details.

LSTM (PTB-LSTM-DEMONGSDM). We train an RNN with LSTM architecture for the PTB language modeling task. Running 5 seeds, DEMON SGDM slightly outperforms other adaptive momentum methods in generalization perplexity, and is competitive with SGDM with learning rate decay. Refer to Figure 3 (*Bottom row, middle plot*) and Table 7 for more details.

Variational AutoEncoder (VAE-MNIST-DEMONGSDM). We train the generative model VAE on the MNIST dataset. Running 5 seeds, DEMON SGDM outperforms all other methods by a 2%-6% generalization error for a small and large number of epochs. Refer to Figure 3 (*Bottom row, right-most plot*) and Table 7 for more details.

A.4 Optimizer hyperparameters

	LSTM		VAE		
	25 epochs	39 epochs	50 epochs	100 epochs	200 epochs
SGDM LR decay	89.59 ± .07	87.57 ± .11	140.51 ± .73	139.54 ± .34	137.33 ± .49
AggMo	89.09 ± .16	89.07 ± .15	139.69 ± .17	139.07 ± .26	137.64 ± .20
QHM	94.47 ± .19	94.44 ± .13	145.84 ± .39	140.92 ± .19	137.64 ± .20
DEMON SGDM	88.33 ± .16	88.32 ± .12	139.32 ± .23	137.51 ± .29	135.95 ± .21

Table 7: PTB-LSTM-DEMONGSDM (perplexity) and VAE-MNIST-DEMONGSDM with no learning rate decay (generalization loss) experiments.

Table 8: Best parameters for CIFAR-10 with ResNet-18.

Optimization method	epochs	η	other parameters
Adam	30	0.001	$\beta_1 = 0.9, \beta_2 = 0.999$
Adam	75	0.001	
Adam	150	0.001	
Adam	300	0.0003	
AMSGrad	30	0.001	$\beta_1 = 0.9, \beta_2 = 0.999$
AMSGrad	75	0.001	
AMSGrad	150	0.001	
AMSGrad	300	0.001	
QHAdam	30	0.001	$\nu_1 = 0.7, \nu_2 = 1.0, \beta_1 = 0.9, \beta_2 = 0.99$
QHAdam	75	0.0003	
QHAdam	150	0.0003	
QHAdam	300	0.0003	
AdamW	30	0.001	$\beta_1 = 0.9, \beta_2 = 0.999, wd = 0.0001$
AdamW	75	0.001	
AdamW	150	0.001	
AdamW	300	0.001	
YellowFin	30	0.001	$\beta_1 = 0$
YellowFin	75	0.001	
YellowFin	150	0.001	
YellowFin	300	0.001	
DEMON Adam	30	0.0001	$\beta_{\text{init}} = 0.9, \beta_2 = 0.999$
DEMON Adam	75	0.0001	
DEMON Adam	150	0.0001	
DEMON Adam	300	0.0001	
AggMo	30	0.03	$\beta = [0, 0.9, 0.99]$
AggMo	75	0.03	
AggMo	150	0.03	
AggMo	300	0.03	
QHM	30	3.0	$\nu = 0.7, \beta = 0.999$
QHM	75	3.0	
QHM	150	3.0	
QHM	300	1.0	
DEMON SGDM	30	0.03	$\beta_{\text{init}} = 0.97, \beta_{\text{final}} = -0.3$
DEMON SGDM	75	0.03	$\beta_{\text{init}} = 0.95, \beta_{\text{final}} = -0.3$
DEMON SGDM	150	0.1	$\beta_{\text{init}} = 0.9, \beta_{\text{final}} = -0.3$
DEMON SGDM	300	0.03	$\beta_{\text{init}} = 0.9, \beta_{\text{final}} = 0$
SGDM	30	0.3	$\beta_1 = 0.9$
SGDM	75	0.1	$\beta_1 = 0.9$
SGDM	150	0.3	$\beta_1 = 0.9$
SGDM	300	0.1	$\beta_1 = 0.9$

B Convergence Analysis

We analyze the global convergence of DEMON SGDM in the convex setting, following [57]. For an objective function f which is convex, continuously differentiable, its gradient $\nabla f(\cdot)$ is Lipschitz continuous with constant L , our goal is to show that $f(\bar{\theta}_T)$ converges to the optimum f^* with decreasing momentum, where $\bar{\theta}_T$ is the average of θ_t for $t = 1, \dots, T$. Our following theorem holds for a constant learning rate and β_t decaying with t .

Theorem 1. Assume that f is convex, continuously differentiable, its gradient $\nabla f(\cdot)$ is Lipschitz continuous with constant L , with a decreasing momentum, but constant step size, as in:

$$\beta_t = \frac{1}{t} \cdot \frac{t+1}{t+2}, \quad \alpha \in \left(0, \frac{2}{3L}\right).$$

We consider the SGDM iteration in non-stochastic settings, where:

$$\theta_{t+1} = \theta_t - \alpha \nabla f(\theta_t) + \beta_t (\theta_t - \theta_{t-1}).$$

Table 9: Best parameters for CIFAR-100 with VGG-16.

Optimization method	epochs	η	other parameters
Adam	75	0.0003	
Adam	150	0.0003	$\beta_1 = 0.9, \beta_2 = 0.999$
Adam	300	0.0003	
AMSGrad	75	0.0003	
AMSGrad	150	0.0003	$\beta_1 = 0.9, \beta_2 = 0.999$
AMSGrad	300	0.0003	
QHAdam	75	0.0003	
QHAdam	150	0.0003	$\nu_1 = 0.7, \nu_2 = 1.0, \beta_1 = 0.9, \beta_2 = 0.99$
QHAdam	300	0.0003	
AdamW	75	0.0003	$\beta_1 = 0.9, \beta_2 = 0.999, wd = 0.01$
AdamW	150	0.0003	$\beta_1 = 0.9, \beta_2 = 0.999, wd = 0.001$
AdamW	300	0.0003	$\beta_1 = 0.9, \beta_2 = 0.999, wd = 0.001$
YellowFin	75	0.1	
YellowFin	150	0.1	$\beta_1 = 0$
YellowFin	300	0.1	
DEMON Adam	75	0.00003	
DEMON Adam	150	0.00003	$\beta_{\text{init}} = 0.9, \beta_2 = 0.999$
DEMON Adam	300	0.00003	
AggMo	75	0.03	
AggMo	150	0.01	$\beta = [0, 0.9, 0.99]$
AggMo	300	0.01	
QHM	75	1.0	
QHM	150	1.0	$\nu = 0.7, \beta = 0.999$
QHM	300	0.3	
DEMON SGDM	75	0.01	
DEMON SGDM	150	0.01	$\beta_{\text{init}} = 0.95, \beta_{\text{final}} = -0.3$
DEMON SGDM	300	0.03	
SGDM	75	0.1	$\beta_1 = 0.9$
SGDM	150	0.03	$\beta_1 = 0.9$
SGDM	300	0.03	$\beta_1 = 0.9$

Then, the sequence $\{\theta_t\}_{t=1}^T$ generated by the SGDM iteration, with decreasing momentum, satisfies:

$$f(\bar{\theta}_T) - f^* \leq \frac{\|\theta_1 - \theta^*\|^2}{T} \left(\frac{3}{4}L + \frac{1}{2\alpha} \right),$$

where $\bar{\theta}_T$ is the Cesaro average of the iterates: $\bar{\theta}_T = \frac{1}{T} \sum_{t=1}^T \theta_t$.

Proof. Let $\beta_t = \frac{1}{t} \cdot \frac{t+1}{t+2}$ and

$$p_t = \frac{1}{t}(\theta_t - \theta_{t-1}).$$

We consider the SGDM iteration in non-stochastic settings, where:

$$\theta_{t+1} = \theta_t - \alpha \nabla f(\theta_t) + \beta_t (\theta_t - \theta_{t-1}).$$

Using the definition of p_t above, one can easily prove that:

$$\theta_{t+1} + p_{t+1} = \left(1 + \frac{1}{t+1}\right)\theta_{t+1} - \frac{1}{t+1}\theta_t = \theta_t + p_t - \frac{\alpha(t+2)}{t+1} \nabla f(\theta_t).$$

Using this expression, we will analyze the term $\|\theta_{t+1} + p_{t+1} - \theta^*\|_2$:

$$\begin{aligned} \|\theta_{t+1} + p_{t+1} - \theta^*\|^2 &= \|\theta_t + p_t - \theta^*\|^2 - \frac{2\alpha(t+2)}{t+1} \langle \theta_t + p_t - \theta^*, \nabla f(\theta_t) \rangle + \left(\frac{\alpha(t+2)}{t+1}\right)^2 \cdot \|\nabla f(\theta_t)\|^2 \\ &= \|\theta_t + p_t - \theta^*\|^2 - \frac{2\alpha(t+2)}{t(t+1)} \langle \theta_t - \theta_{t-1}, \nabla f(\theta_t) \rangle \\ &\quad - \frac{2\alpha(t+2)}{t+1} \langle \theta_t - \theta^*, \nabla f(\theta_t) \rangle + \left(\frac{\alpha(t+2)}{t+1}\right)^2 \cdot \|\nabla f(\theta_t)\|^2 \end{aligned}$$

Table 10: Best parameters for STL10 with Wide ResNet 16-8.

Optimization method	epochs	η	other parameters
Adam	50	0.001	$\beta_1 = 0.9, \beta_2 = 0.999$
Adam	100	0.0003	
Adam	200	0.0003	
AMSGrad	50	0.0003	$\beta_1 = 0.9, \beta_2 = 0.999$
AMSGrad	100	0.0003	
AMSGrad	200	0.0003	
QHAdam	50	0.0003	$\nu_1 = 0.7, \nu_2 = 1.0, \beta_1 = 0.9, \beta_2 = 0.99$
QHAdam	100	0.0003	
QHAdam	200	0.0003	
AdamW	50	0.0003	$\beta_1 = 0.9, \beta_2 = 0.999, wd = 0.001$
AdamW	100	0.0003	
AdamW	200	0.0003	
YellowFin	50	0.1	$\beta_1 = 0$
YellowFin	100	0.1	
YellowFin	200	0.1	
DEMON Adam	50	0.00003	$\beta_{init} = 0.9, \beta_2 = 0.999$
DEMON Adam	100	0.00003	
DEMON Adam	200	0.00003	
AggMo	50	0.1	$\beta = [0, 0.9, 0.99]$
AggMo	100	0.1	
AggMo	200	0.1	
QHM	50	1.0	$\nu = 0.7, \beta = 0.999$
QHM	100	3.0	
QHM	200	3.0	
DEMON SGDM	50	0.1	$\beta_{init} = 0.9$
DEMON SGDM	100	0.1	
DEMON SGDM	200	0.1	
SGDM	50	0.1	$\beta_1 = 0.9$
SGDM	100	0.1	$\beta_1 = 0.9$
SGDM	200	0.1	$\beta_1 = 0.9$

Table 11: Best parameters for Tiny ImageNet with ResNet-56.

Optimization method	epochs	η	other parameters
Adam	20	0.001	$\beta_1 = 0.9, \beta_2 = 0.999$
Adam	40	0.0003	
DEMON Adam	20	0.001	$\beta_{init} = 0.9, \beta_2 = 0.999$
DEMON Adam	40	0.0001	
DEMON SGDM	20	0.1	$\beta_{init} = 0.93, \beta_{final} = 0.0$
DEMON SGDM	40	0.1	$\beta_{init} = 0.9, \beta_{final} = 0.0$
SGDM	20	0.1	$\beta_1 = 0.9$
SGDM	40	0.1	$\beta_1 = 0.9$

Table 12: Best parameters for PTB with LSTM architecture.

Optimization method	epochs	η	other parameters
Adam	25	0.0003	$\beta_1 = 0.9, \beta_2 = 0.999$
Adam	39	0.0003	
AMSGrad	25	0.001	$\beta_1 = 0.9, \beta_2 = 0.999$
AMSGrad	39	0.001	
QHAdam	25	0.0003	$\nu_1 = 0.7, \nu_2 = 1.0, \beta_1 = 0.9, \beta_2 = 0.999$
QHAdam	39	0.0003	
AdamW	25	0.001	$\beta_1 = 0.9, \beta_2 = 0.999, wd = 0.00005$
AdamW	39	0.001	
YellowFin	25	0.1	$\beta_1 = 0$
YellowFin	39	0.1	
DEMON Adam	25	0.0001	$\beta_{init} = 0.9, \beta_2 = 0.999$
DEMON Adam	39	0.0001	
AggMo	25	0.03	$\beta = [0, 0.9, 0.99]$
AggMo	39	0.03	
QHM	25	1.0	$\nu = 0.7, \beta = 0.999$
QHM	39	1.0	
DEMON SGDM	25	1.0	$\beta_{init} = 0.5, \beta_{final} = -0.5$ $\beta_{init} = 0.3, \beta_{final} = -0.5$
DEMON SGDM	39	1.0	
SGDM	25	0.1	$\beta_1 = 0.9, \text{smooth learning rate decay}$ $\beta_1 = 0.0, \text{smooth learning rate decay}$
SGDM	39	1.0	

Since f is convex, continuously differentiable, its gradient is Lipschitz continuous with constant L , then

$$\frac{1}{L} \|\nabla f(\theta_t)\|^2 \leq \langle \theta_t - \theta^*, \nabla f(\theta_t) \rangle, \quad (2)$$

$$f(\theta_t) - f^* + \frac{1}{2L} \|\nabla f(\theta_t)\|^2 \leq \langle \theta_t - \theta^*, \nabla f(\theta_t) \rangle, \quad (3)$$

$$f(\theta_t) - f(\theta_{t-1}) \leq \langle \theta_t - \theta_{t-1}, \nabla f(\theta_t) \rangle. \quad (4)$$

Substituting the above inequalities leads to

$$\begin{aligned} \|\theta_{t+1} + p_{t+1} - \theta^*\|^2 &\leq \|\theta_t + p_t - \theta^*\|^2 - \frac{2\alpha(t+2)}{t(t+1)} (f(\theta_t) - f(\theta_{t-1})) \\ &\quad - 2\alpha \frac{(1-\lambda)(t+2)}{L(t+1)} \cdot \|\nabla f(\theta_t)\|^2 - 2\alpha \lambda \frac{t+2}{t+1} (f(\theta_t) - f^*) \\ &\quad - \left(\alpha \frac{\lambda(t+2)}{L(t+1)} \right) \cdot \|\nabla f(\theta_t)\|^2 + \left(\frac{\alpha(t+2)}{t+1} \right)^2 \cdot \|\nabla f(\theta_t)\|^2 \end{aligned}$$

where $\lambda \in (0, 1]$ is a parameter weighting (2) and (3). Grouping together terms yields

$$\begin{aligned} &\left(\frac{2\alpha(t+2)}{t(t+1)} + \frac{2\alpha\lambda(t+2)}{t+1} \right) (f(\theta_t) - f^*) + \|\theta_{t+1} + p_{t+1} - \theta^*\|^2 \\ &\leq \frac{2\alpha(t+2)}{t(t+1)} (f(\theta_{t-1}) - f^*) + \|\theta_t + p_t - \theta^*\|^2 \\ &\quad + \frac{\alpha(t+2)}{t+1} \left(\frac{\alpha(t+2)}{t+1} - \frac{2(1-\lambda)}{L} - \frac{\lambda}{L} \right) \|\nabla f(\theta_t)\|^2. \end{aligned}$$

The last term is non-positive when $\alpha \in [0, \frac{t+1}{t+2}(\frac{2-\lambda}{L})]$ so it can be dropped. Summing over $t = 1, \dots, T$ yields

$$\begin{aligned} 2\alpha\lambda \sum_{t=1}^T \frac{t+2}{t+1} (f(\theta_t) - f^*) + \sum_{t=1}^T \left(\frac{2\alpha(t+2)}{t(t+1)} (f(\theta_t) - f^*) + \|\theta_{t+1} + p_{t+1} - \theta^*\|^2 \right) \\ \leq \sum_{t=1}^T \left(\frac{2\alpha(t+2)}{t(t+1)} (f(\theta_{t-1}) - f^*) + \|\theta_t + p_t - \theta^*\|^2 \right), \end{aligned}$$

implying that:

$$2\alpha\lambda \sum_{t=1}^T \frac{t+2}{t+1} (f(\theta_t) - f^*) \leq 3\alpha(f(\theta_1) - f^*) + \|\theta_1 - \theta^*\|^2.$$

Table 13: Best parameters for MNIST with VAE.

Optimization method	epochs	η	other parameters
Adam	50	0.001	$\beta_1 = 0.9, \beta_2 = 0.999$
Adam	100	0.001	
Adam	200	0.001	
AMSGrad	50	0.001	$\beta_1 = 0.9, \beta_2 = 0.999$
AMSGrad	100	0.001	
AMSGrad	200	0.001	
QHAdam	50	0.001	$\nu_1 = 0.7, \nu_2 = 1.0, \beta_1 = 0.9, \beta_2 = 0.99$
QHAdam	100	0.001	
QHAdam	200	0.001	
AdamW	50	0.001	$\beta_1 = 0.9, \beta_2 = 0.999, wd = 0.0001$
AdamW	100	0.001	
AdamW	200	0.001	
YellowFin	50	0.0001	$\beta_1 = 0$
YellowFin	100	0.0001	
YellowFin	200	0.0001	
DEMON Adam	50	0.0001	$\beta_{\text{init}} = 0.9, \beta_2 = 0.999$
DEMON Adam	100	0.0001	
DEMON Adam	200	0.0001	
AggMo	50	0.000003	$\beta = [0, 0.9, 0.99]$
AggMo	100	0.000003	
AggMo	200	0.000003	
QHM	50	0.0001	$\nu = 0.8, \beta = 0.999$
QHM	100	0.0001	
QHM	200	0.0001	
DEMON SGDM	50	0.0003	$\beta_{\text{init}} = 0.97$
DEMON SGDM	100	0.0003	
DEMON SGDM	200	0.0003	
SGDM	50	0.00001	$\beta_1 = 0.9$
SGDM	100	0.00001	$\beta_1 = 0.9$
SGDM	200	0.00001	$\beta_1 = 0.9$

Table 14: Best parameters for FMNIST with Capsule Network.

Optimization method	epochs	η	other parameters
Adam	50	0.001	$\beta_1 = 0.9, \beta_2 = 0.999$
Adam	100	0.001	
AMSGrad	50	0.001	$\beta_1 = 0.9, \beta_2 = 0.999$
AMSGrad	100	0.001	
QHAdam	50	0.0003	$\nu_1 = 0.7, \nu_2 = 1.0, \beta_1 = 0.9, \beta_2 = 0.999$
QHAdam	100	0.0003	
AdamW	50	0.001	$\beta_1 = 0.9, \beta_2 = 0.999, wd = 0.0001$
AdamW	100	0.001	
YellowFin	50	0.001	$\beta_1 = 0$
YellowFin	100	0.001	
DEMON Adam	50	0.001	$\beta_{\text{init}} = 0.9, \beta_2 = 0.999$
DEMON Adam	100	0.001	

Since:

$$2\alpha\lambda \sum_{t=1}^T (f(\theta_t) - f^*) \leq 2\alpha\lambda \sum_{t=1}^T \frac{t+2}{t+1} (f(\theta_t) - f^*) \leq 3\alpha\lambda \sum_{t=1}^T (f(\theta_t) - f^*),$$

we further have:

$$3\alpha\lambda \sum_{t=1}^T (f(\theta_t) - f^*) \leq \frac{3}{2} \left(3\alpha(f(\theta_1) - f^*) + \|\theta_1 - \theta^*\|^2 \right).$$

Due to the convexity of f ,

$$f(\bar{\theta}_t) \leq \frac{1}{T} \sum_{t=1}^T f(\theta_t),$$

observe that

$$f(\bar{\theta}_T) - f^* \leq \frac{1}{T} \sum_{t=1}^T (f(\theta_t) - f^*) \leq \frac{1}{3\alpha\lambda T} \left(\frac{9}{2}\alpha(f(\theta_1) - f^*) + \frac{3}{2}\|\theta_1 - \theta^*\|^2 \right).$$

Since $f(\theta_1) - f^* \leq \frac{\lambda}{2}\|\theta_1 - \theta^*\|^2$ by Lipschitz continuous gradients, setting $\lambda = 1$ and observing $(t+1)/(t+2) \geq 2/3$ gives the result.

For DEMON Adam, we observe it lies within the definition of Generic Adam in [58], and inherits the non-convex results. We leave this as an exercise to the reader.

C Linear Regression

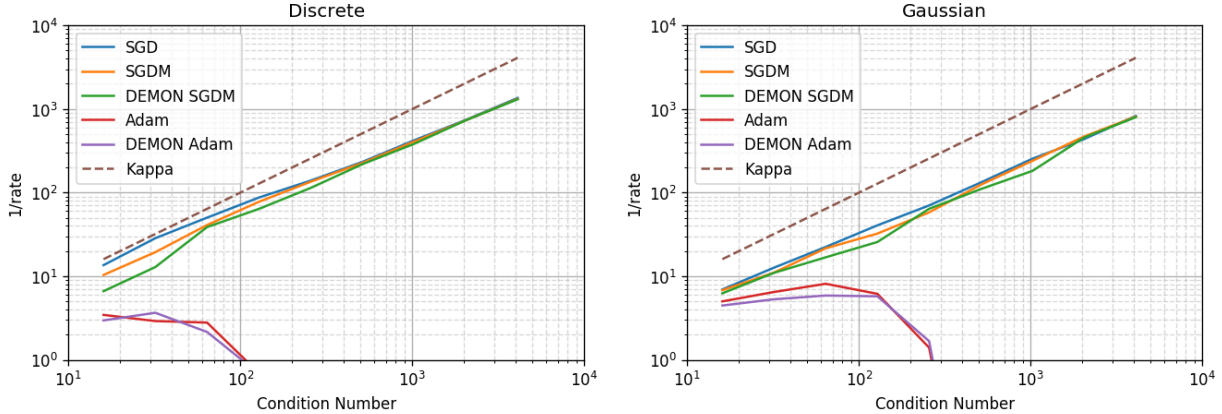


Figure 4: Linear regression with $1/\text{rate}$ vs κ (Condition Number). Left: Discrete. Right: Gaussian.

We replicate the linear regression setting in [45] and summarize the key details here. We consider two different classes of linear regression problems in two dimensions, where κ is the condition number and samples are (a, b) , namely:

Discrete: $a = e_1$ with probability 0.5, and $a = \frac{2}{\kappa}e_2$ w.p. 0.5; e_i is the i -th standard basis vector.

Gaussian: $a \in \mathbb{R}^2$ distributed as a Gaussian random vector with covariance matrix $\begin{pmatrix} 1 & 0 \\ 0 & \frac{1}{\kappa} \end{pmatrix}$.

We evaluate SGD, SGDM, DEMON SGDM, Adam, and DEMON Adam, tuning with a grid search. We fix a randomly generated θ^* , and let $b = \langle \theta^*, a \rangle$. κ is varied from 2^4 to 2^{12} in powers of 2 and for each setting we run 100 independent trials for $t = 5\kappa$ iterations, considering only those that converged. Following [45], the algorithm is considered to converge if no error in the second half of iterations exceeds starting error. Performance is measured using $\text{rate} = \frac{\log(f(\theta_1)) - \log(f(\theta_t))}{t}$ and we compute the rate for different κ . Results are given in Figure 4: What is apparent is that the convergence rate is preserved when we decrease the momentum parameter, despite the fact that theory dictates the opposite in convex scenarios.

Table 15: VGG16-CIFAR100-DEMONGSDM and WRN-STL10-DEMONGSDM generalization error. The number of epochs was predefined before the execution.

	VGG-16			Wide Residual 16-8		
	75 epochs	150 epochs	300 epochs	50 epochs	100 epochs	200 epochs
SGD ELR	36.82 ± .68	30.34 ± .30	29.81 ± .31	20.90 ± .47	17.53 ± .32	15.37 ± .51
DEMON SGDM	33.08 ± .49	30.22 ± .50	27.71 ± .05	19.45 ± .20	15.98 ± .40	13.67 ± .13

Table 16: PTB-LSTM-DEMONGSDM (perplexity) and VAE-MNIST-DEMONGSDM (generalization loss) experiments.

	LSTM			VAE		
	25 epochs	39 epochs	50 epochs	100 epochs	200 epochs	
SGD ELR	inf	inf	inf	inf	inf	
DEMON SGDM	88.33 ± .16	88.32 ± .12	139.32 ± .23	137.51 ± .29	135.95 ± .21	

D Demon and effective learning rate

In this section, we present results of Demon against the effective learning rate adjusted SGD (SGD ELR). The effective learning rate is proposed to approximate SGDM with SGD, where the learning rate is adjusted with a factor of $1/(1 - m)$ and m is the momentum coefficient. However, the results in Tables 15, 16, and 17 demonstrate that DEMON cannot be accurately approximated with an effective learning rate adjusted SGD. For both settings in Table 16 (PTB-LSTM-DEMONGSDM and VAE-MNIST-DEMONGSDM), SGD ELR causes learning to diverge. In Table 15, there exists a 1-3% generalization error gap for VGG16-CIFAR100-DEMONGSDM and WRN-STL10-DEMONGSDM. In Table 17, there exists a 1% generalization gap for RN18-CIFAR10-DEMONGSDM.

E Additional plots

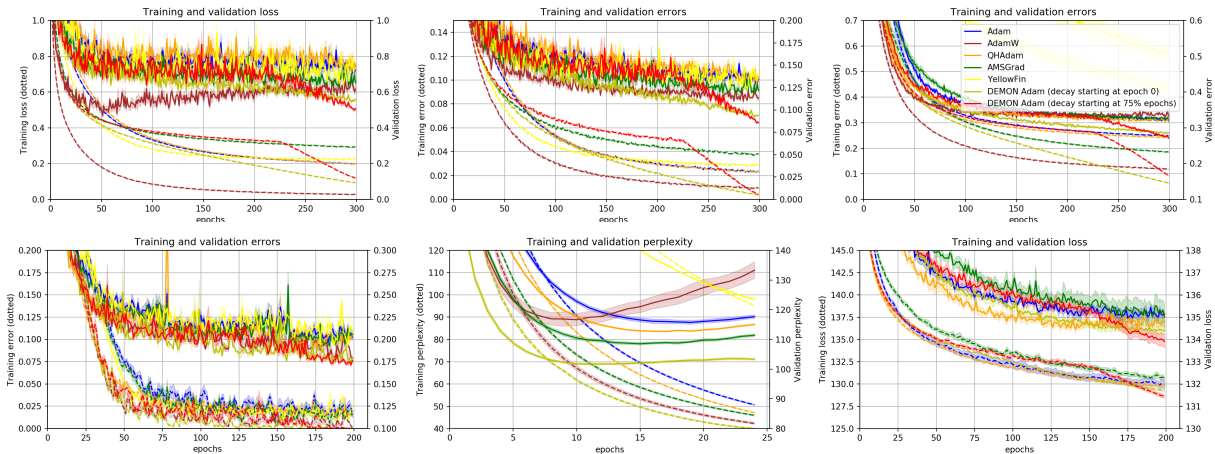


Figure 5: Top row, two left-most plots: RN18-CIFAR10-DEMONAdam for 300 epochs. Top row, right-most plot: VGG16-CIFAR100-DEMONAdam for 300 epochs. Bottom row, left-most plot: WRN-STL10-DEMONAdam for 200 epochs. Bottom row, middle plot: PTB-LSTM-DEMONAdam for 25 epochs. Bottom row, right-most plot: VAE-MNIST-DEMONAdam for 200 epochs. Dotted and solid lines represent training and generalization metrics respectively. Shaded bands represent one standard deviation.

Table 17: RN18-CIFAR10-DEMONGSDM generalization error. The number of epochs was predefined before the execution of the algorithms.

	30 epochs	75 epochs	150 epochs	300 epochs
SGD ELR	11.82 ± .13	9.46 ± .25	8.72 ± .06	8.46 ± .19
DEMON SGDM	10.39 ± .39	8.74 ± .28	7.82 ± .27	7.58 ± .04

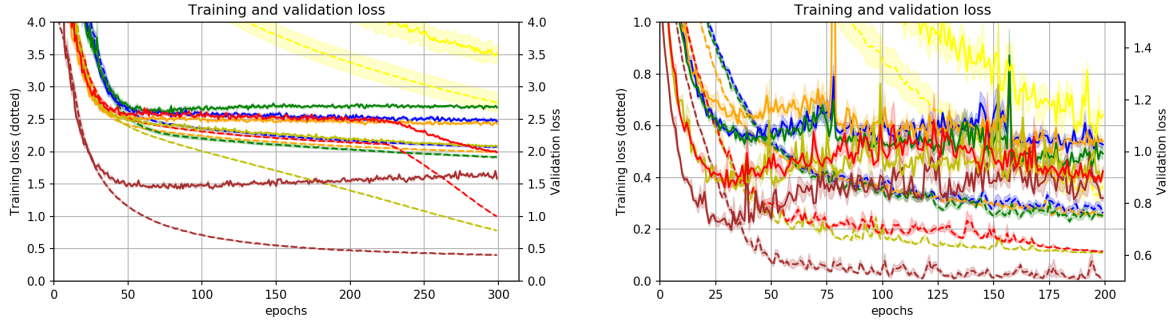


Figure 6: Additional empirical results on adaptive learning rate methods. Left plot: VGG16-CIFAR100-DEMONAdam for 300 epochs. Right plot: WRN-STL10-DEMONAdam for 200 epochs. Dotted and solid lines represent training and generalization metrics respectively. Shaded bands represent 1 standard deviation.

F Padam and OneCycle preliminary results

In this section, we present preliminary results on Padam [40] and OneCycle [47] on several tasks. We conducted preliminary studies of Padam for the settings of ResNet18 on CIFAR10 with 300 epochs, VGG16 on CIFAR100 with 150 epochs, and Variational AutoEncoder on MNIST with 50 epochs.

For RN18-CIFAR10, following the Padam paper, we try learning rate in $[0.1, 0.03, 0.01, 0.003, 0.001, 0.0003]$, $p \in [1/4, 1/8, 1/16]$, $\beta_1 = 0.9$, $\beta_2 = 0.999$. The lowest test error is attained with learning rate 0.01 and $p = 1/4$, at $12.13 \pm .70$. Demon Adam achieves significantly lower test error at $8.44 \pm .05$.

For VGG16-CIFAR100 and Padam, we try learning rate in $[0.1, 0.03, 0.01, 0.003, 0.001, 0.0003]$, $p \in [1/4, 1/8, 1/16]$, $\beta_1 = 0.9$, $\beta_2 = 0.999$. The lowest test error is attained with learning rate 0.03 and $p = 1/16$, at $34.38 \pm .71$. Demon Adam, again, achieves significantly lower test error at $28.84 \pm .18$.

For VAE-MNIST and Padam, we try learning rate in $[0.003, 0.001, 0.0003, 0.0001]$, exponent $p \in [0.4, 0.25, 0.125, 0.0625]$ and $\beta_1 = 0.9$, $\beta_2 = 0.999$. The lowest validation loss is attained with learning rate 0.001 and $p = 0.4$, with a loss value of $137.37 \pm .75$. For this task, Demon Adam achieves $134.46 \pm .17$, substantially better.

We also conducted preliminary studies of 1cycle with momentum SGD for the settings of ResNet18 on CIFAR10 for 300 epochs and VGG16 on CIFAR100 for 150 epochs.

Following the suggestions in the paper, for RN18-CIFAR10 we try all combinations of maximum learning rate in $[3.0, 1.0, 0.3, 0.1, 0.03, 0.01]$, maximum momentum in $[0.97, 0.95, 0.9]$, minimum momentum in $[0.85, 0.8]$, batch size in $[128, 256, 512]$, with minimum learning rate = $0.1 \cdot$ maximum learning rate. The lowest test error is achieved with maximum learning rate 1.0, maximum momentum 0.95, minimum momentum 0.85, batch size 512, achieving $7.65 \pm .13$. Demon SGDM, with no tuning, achieves $7.58 \pm .04$.

For VGG16-CIFAR100, we try all combinations of maximum learning rate in $[1.0, 0.3, 0.1, 0.03]$, maximum momentum in $[0.97, 0.95, 0.9]$, minimum momentum in $[0.85, 0.8]$, batch size in $[128, 256, 512]$, with minimum learning rate = $0.1 \cdot$ maximum learning rate. The lowest test error is achieved with maximum learning rate 0.1, maximum momentum 0.95, minimum momentum 0.85, batch size 512, achieving 32.05 ± 1.05 . In comparison, Demon SGDM, with no tuning, achieves significantly lower at $30.22 \pm .50$.

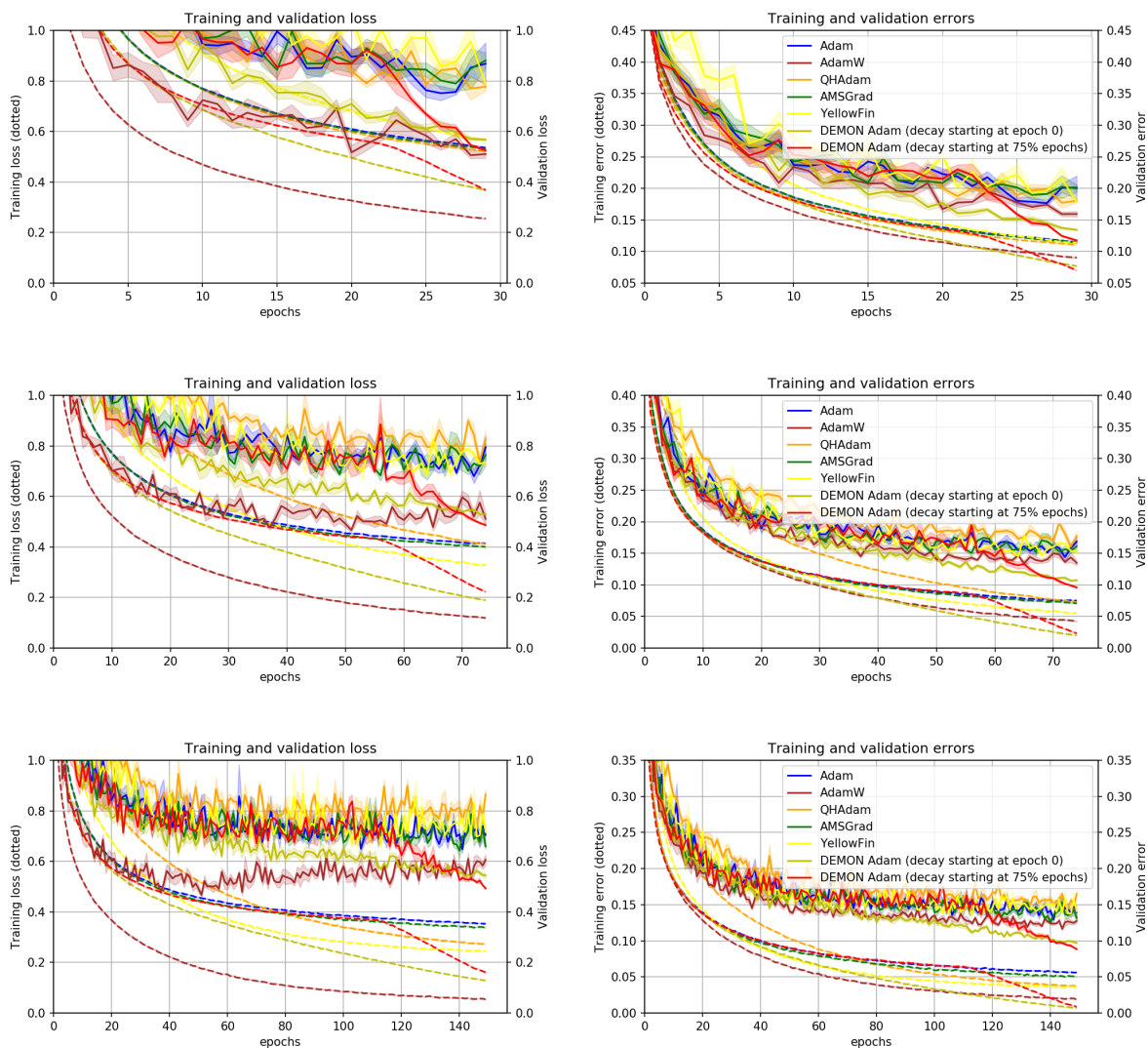


Figure 7: Additional empirical results on RN18-CIFAR10-DEMONAdam. Top row: 30 epochs. Middle row: 75 epochs. Bottom row: 150 epochs. Dotted and solid lines represent training and generalization metrics respectively. Shaded bands represent 1 standard deviation.

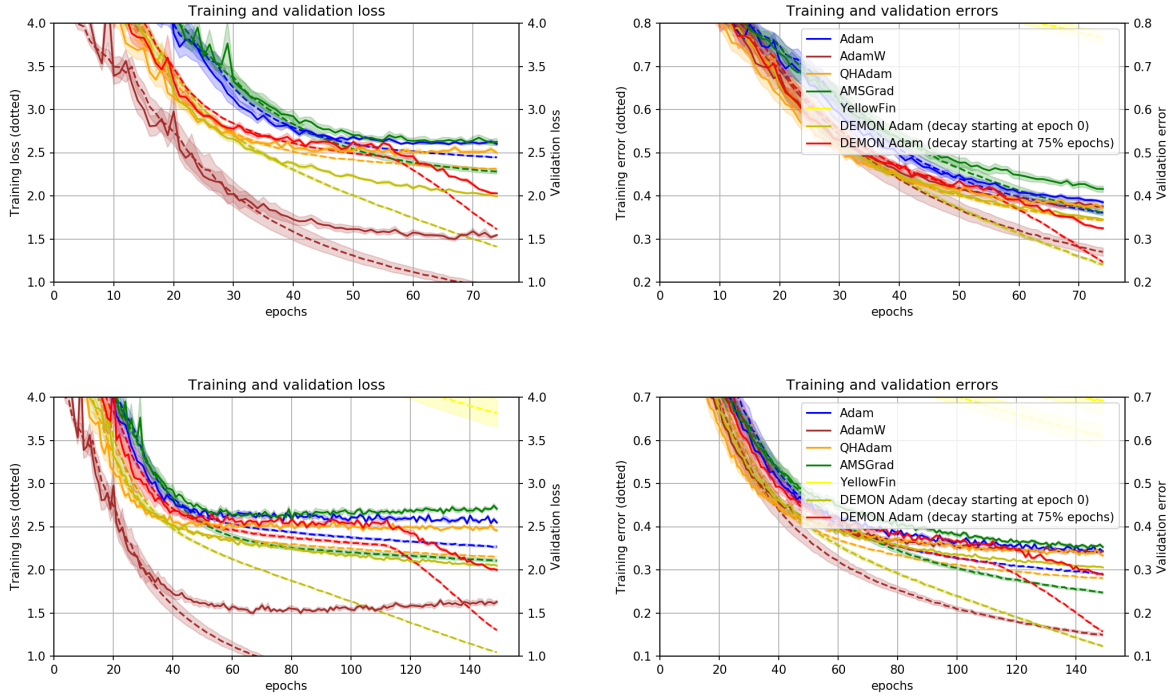


Figure 8: Additional empirical results on VGG16-CIFAR100-DEMONAdam. Top row: 75 epochs. Bottom row: 150 epochs. Dotted and solid lines represent training and generalization metrics respectively. Shaded bands represent 1 standard deviation.

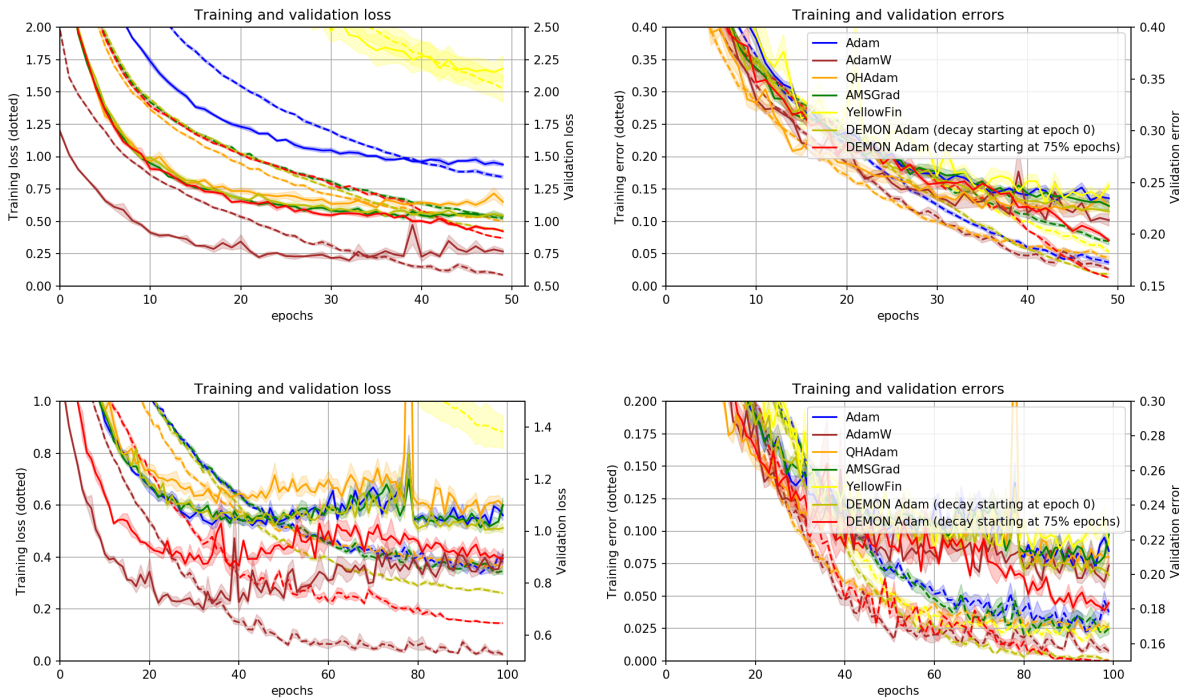


Figure 9: Additional empirical results on WRN-STL10-DEMONAdam. Top row: 50 epochs. Bottom row: 100 epochs. Dotted and solid lines represent training and generalization metrics respectively. Shaded bands represent 1 standard deviation.

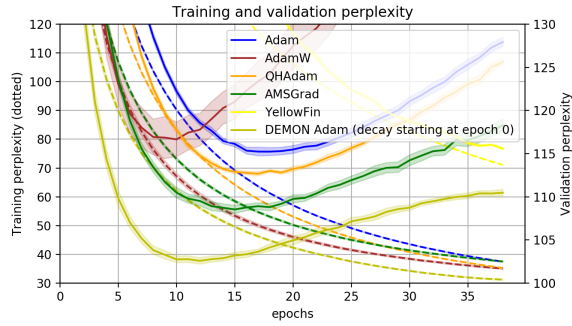


Figure 10: Additional empirical results on PTB-LSTM-DEMONAdam for 39 epochs. Dotted and solid lines represent training and generalization metrics respectively. Shaded bands represent 1 standard deviation.

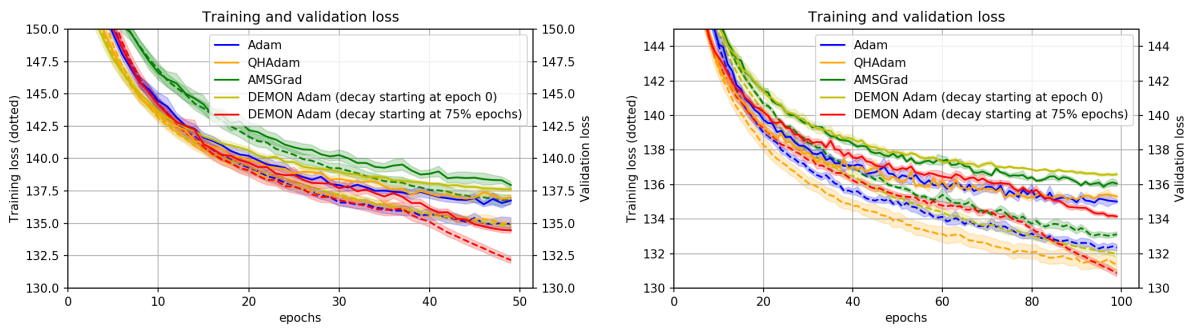


Figure 11: Additional empirical results on VAE-MNIST-DEMONAdam. Left: 50 epochs. Right: 100 epochs. Dotted and solid lines represent training and generalization metrics respectively. Shaded bands represent 1 standard deviation.

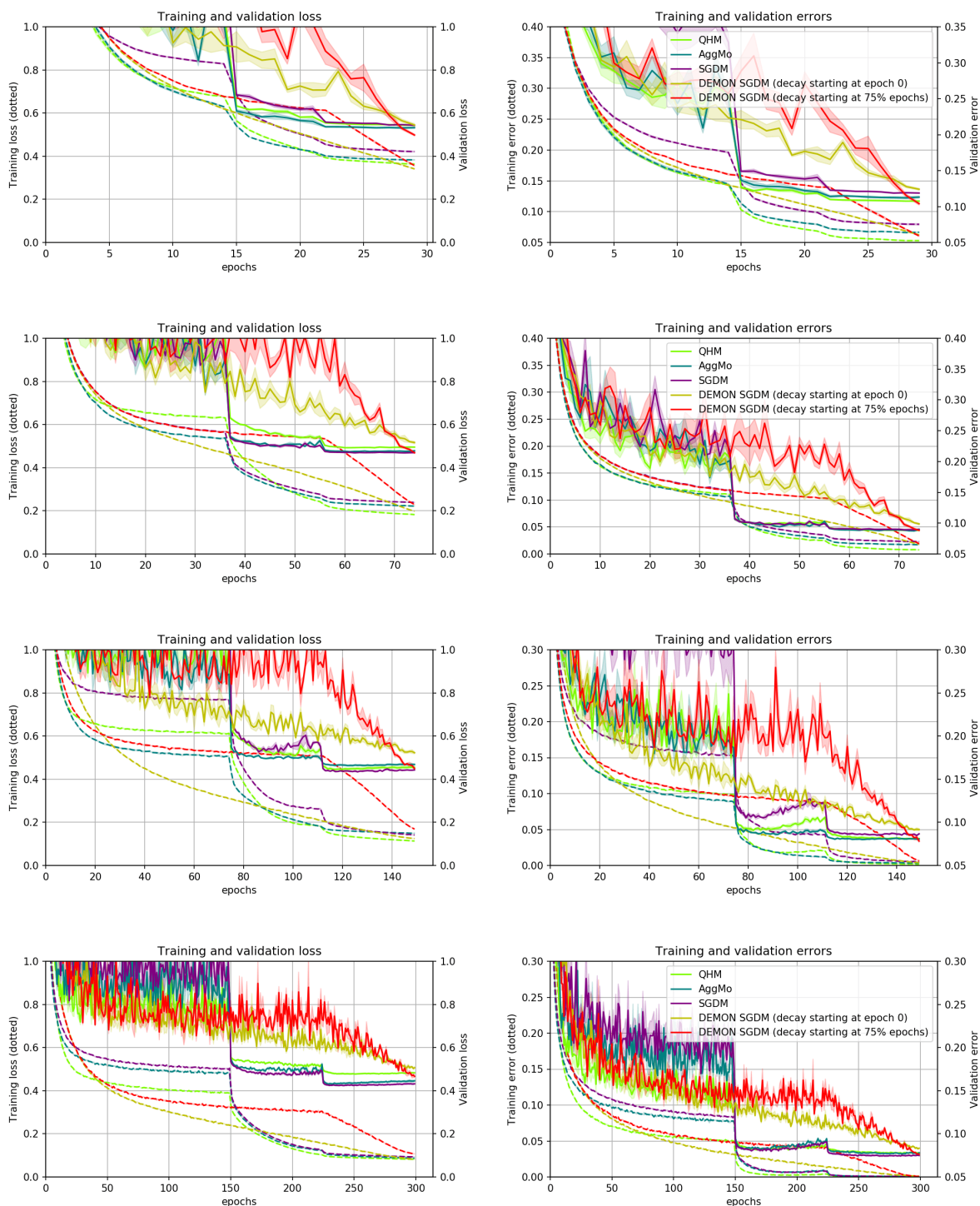


Figure 12: Additional empirical results on RN18-CIFAR10-DEMONGSDM. Top row: 30 epochs. Middle upper row: 75 epochs. Middle lower row: 150 epochs. Bottom row: 300 epochs. Dotted and solid lines represent training and generalization metrics respectively. Shaded bands represent 1 standard deviation.

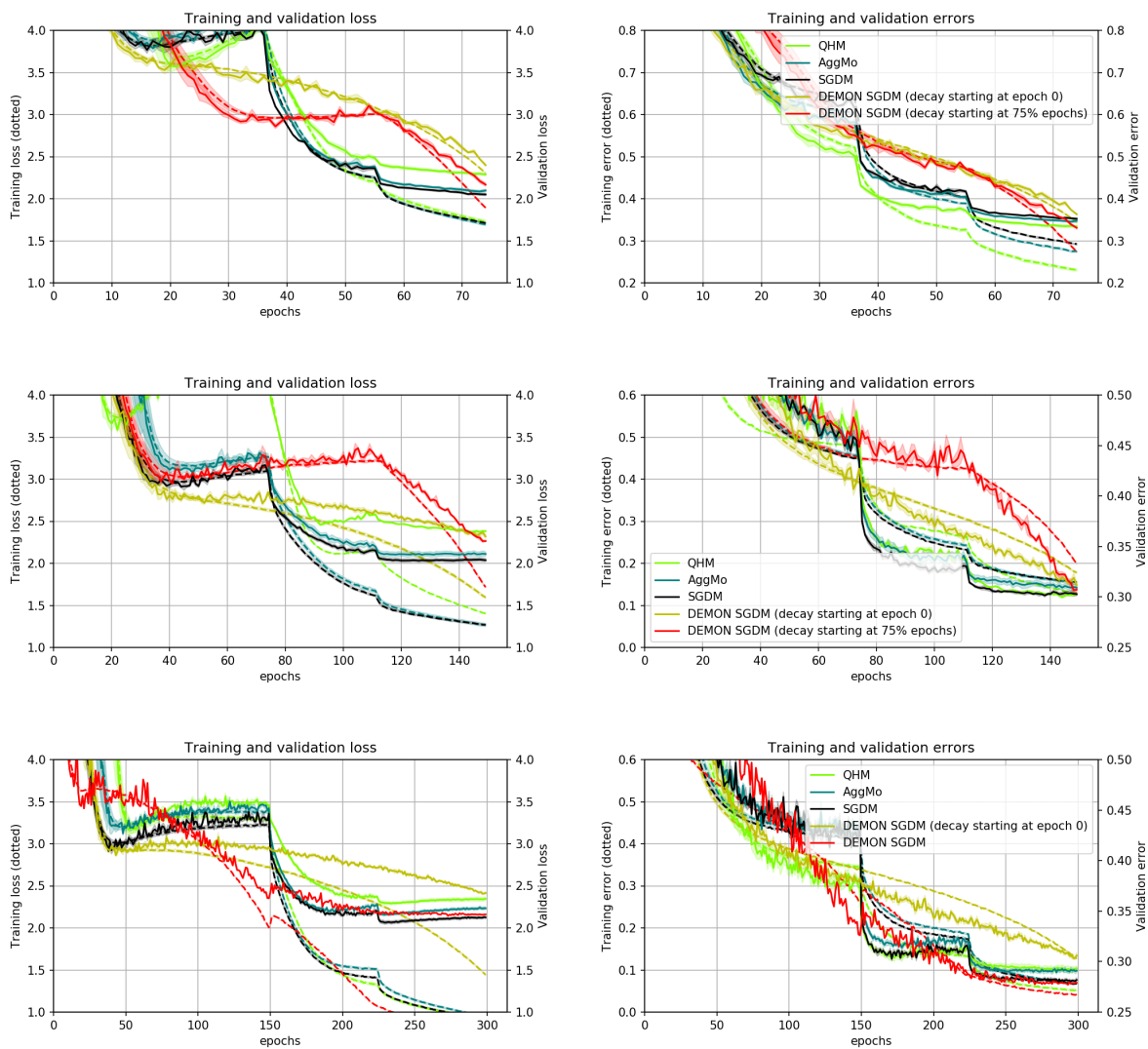


Figure 13: Additional empirical results on VGG16-CIFAR100-DEMONSGDM. Top row: 75 epochs. Middle row: 150 epochs. Bottom row: 300 epochs. Dotted and solid lines represent training and generalization metrics respectively. Shaded bands represent 1 standard deviation.

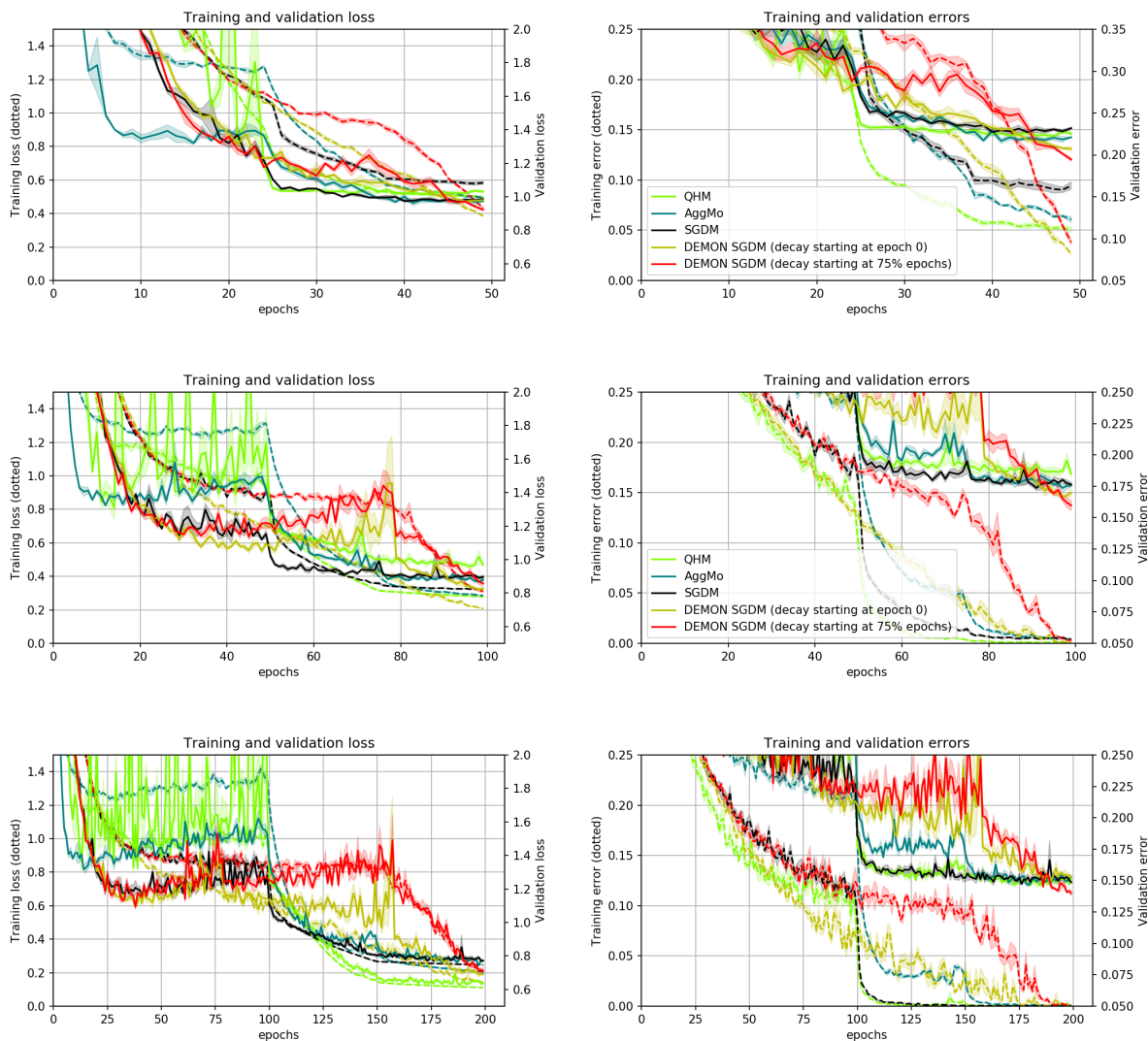


Figure 14: Additional empirical results on WRN-STL10-DEMONSGDM. Top row: 50 epochs. Middle row: 100 epochs. Bottom row: 200 epochs. Dotted and solid lines represent training and generalization metrics respectively. Shaded bands represent 1 standard deviation.

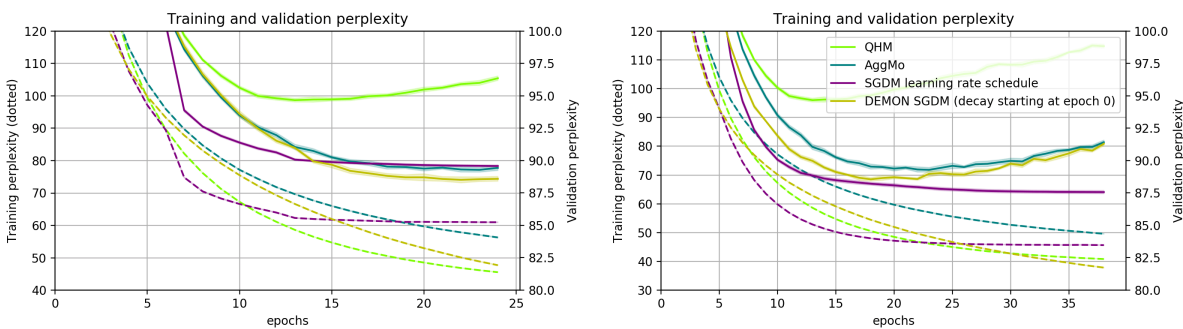


Figure 15: Additional empirical results on PTB-LSTM-DEMONSGDM. Left: 25 epochs. Right: 39 epochs. Dotted and solid lines represent training and generalization metrics respectively. Shaded bands represent 1 standard deviation.

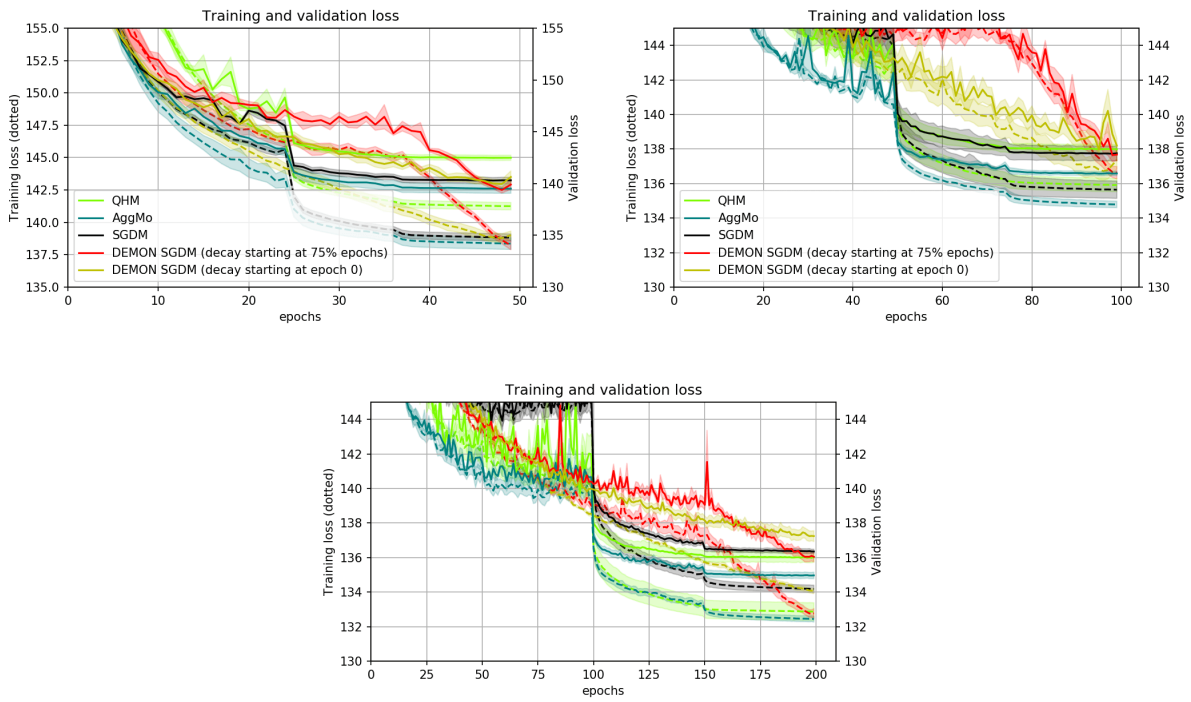


Figure 16: Additional empirical results on VAE-MNIST-DEMONGSDM. Left: 50 epochs. Right: 100 epochs. Bottom: 200 epochs. Dotted and solid lines represent training and generalization metrics respectively. Shaded bands represent 1 standard deviation.